AD

ER 2391

ANALYTICAL, EXPERIMENTAL AND MECHANICAL
EVALUATION OF FREE ROTATING VANELESS DIFFUSERS

Final Report
Edited By

C. Rodgers

May 1972

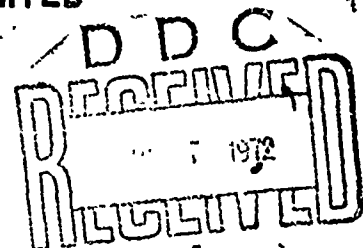U. S. Army Mobility Equipment Research and Development Center
Fort Belvoir, Virginia

Contract DAAK02-71-C-0189

Solar Division of International Harvester Company
2200 Pacific Highway, San Diego, California 92112

DISTRIBUTION OF THIS REPORT IS UNLIMITED

DDC

RECEIVED

1972

A

98

Destroy this report when it is no longer needed.   Do not return it to originator.

DOCUMENT CONTROL DATA - R&D

(Security classification of title body of abstract and indexing annotation must be entered when the overall report is classified)

1 ORIGINATING ACTIVITY *(Corporate author)*	2a REPORT SECURITY CLASSIFICATION
Solar, Division of International Harvester Company 2200 Pacific Highway San Diego, California 92112	UNCLASSIFIED
	2b GROUP N/A

3 REPORT TITLE

Analytical, Experimental and Mechanical Evaluation of
Free Rotating Vaneless Diffusers

4 DESCRIPTIVE NOTES *(Type of report and inclusive dates)*

Final Report, Feb 1971 - Feb 1972

5 AUTHOR(S) *(Last name, first name, initial)*

C. Rodgers and H. Mnew

6 REPORT DATE	7a TOTAL NO. OF PAGES	7b NO OF REFS
May 1972	102	5

8a CONTRACT OR GRANT NO. DAAK02-71-C-0189	9a ORIGINATOR'S REPORT NUMBER(S)
b PROJECT NO. DA Project 1G663702DG11-01	ER-2391
c	9b OTHER REPORT NO(S) *(Any other numbers that may be assigned this report)*
d	

10 AVAILABILITY/LIMITATION NOTICES

Distribution of this document is unlimited.

11 SUPPLEMENTARY NOTES	12 SPONSORING MILITARY ACTIVITY U.S. Army Mobility Equipment Research and Development Center Fort Belvoir, Virginia

13 ABSTRACT

Experimental testing of a model free rotating vaneless diffuser rig to determine diffuser loss coefficients and static pressure recovery under braked and free rotating conditions was conducted. The rig was operated at entry Mach numbers up to unity with both vaned and vaneless diffusers installed downstream. Two rotating diffuser widths were tested.

A significant improvement in diffuser performance was achieved under free rotating conditions, even though large wakes generated by upstream stationary swirl nozzles were present. Overall static pressure recovery for the complete diffusion system increased approximately 20% at free rotating conditions corresponding to a tangential velocity ratio (diffuser/incident stream) of 0.43. The total pressure loss reduction between braked and rotating conditions correlated with theoretical studies. A mechanical design study to examine methods of integrating the rotating diffuser into a complete gas turbine was also conducted and a feasible preliminary design identified. ( )

14		LINK A		LINK B		LINK C	
	KEY WORDS	ROLE	WT	ROLE	WT	ROLE	WT
Centrifugal Compressor							
Diffuser							
High Pressure Ratio							
Mach Number							
Gas Turbine							
Skin Friction							

INSTRUCTIONS

1. ORIGINATING ACTIVITY: Enter the name and address of the contractor, subcontractor, grantee, Department of Defense activity or other organization (corporate author) issuing the report.

2a. REPORT SECURITY CLASSIFICATION: Enter the overall security classification of the report. Indicate whether "Restricted Data" is included. Marking is to be in accordance with appropriate security regulations.

2b. GROUP: Automatic downgrading is specified in DoD Directive 5200.10 and Armed Forces Industrial Manual. Enter the group number. Also, when applicable, show that optional markings have been used for Group 3 and Group 4 as authorized.

3. REPORT TITLE: Enter the complete report title in all capital letters. Titles in all cases should be unclassified. If a meaningful title cannot be selected without classification, show title classification in all capitals in parenthesis immediately following the title.

4. DESCRIPTIVE NOTES: If appropriate, enter the type of report, e.g., interim, progress, summary, annual, or final. Give the inclusive dates when a specific reporting period is covered.

5. AUTHOR(S): Enter the name(s) of author(s) as shown on or in the report. Enter last name, first name, middle initial. If military, show rank and branch of service. The name of the principal author is an absolute minimum requirement.

6. REPORT DATE: Enter the date of the report as day, month, year; or month, year. If more than one date appears on the report, use date of publication.

7a. TOTAL NUMBER OF PAGES: The total page count should follow normal pagination procedures, i.e., enter the number of pages containing information.

7b. NUMBER OF REFERENCES: Enter the total number of references cited in the report.

8a. CONTRACT OR GRANT NUMBER: If appropriate, enter the applicable number of the contract or grant under which the report was written.

8b, 8c, & 8d. PROJECT NUMBER: Enter the appropriate military department identification, such as project number, subproject number, system numbers, task number, etc.

9a. ORIGINATOR'S REPORT NUMBER(S): Enter the official report number by which the document will be identified and controlled by the originating activity. This number must be unique to this report.

9b. OTHER REPORT NUMBER(S): If the report has been assigned any other report numbers (either by the originator or by the sponsor), also enter this number(s).

10. AVAILABILITY/LIMITATION NOTICES: Enter any limitations on further dissemination of the report, other than those imposed by security classification, using standard statements such as:

(1) "Qualified requesters may obtain copies of this report from DDC."

(2) "Foreign announcement and dissemination of this report by DDC is not authorized."

(3) "U. S. Government agencies may obtain copies of this report directly from DDC. Other qualified DDC users shall request through

_____."

(4) "U. S. military agencies may obtain copies of this report directly from DDC. Other qualified users shall request through

_____."

(5) "All distribution of this report is controlled. Qualified DDC users shall request through

_____."

If the report has been furnished to the Office of Technical Services, Department of Commerce, for sale to the public, indicate this fact and enter the price, if known.

11. SUPPLEMENTARY NOTES: Use for additional explanatory notes.

12. SPONSORING MILITARY ACTIVITY: Enter the name of the departmental project office or laboratory sponsoring (paying for) the research and development. Include address.

13. ABSTRACT: Enter an abstract giving a brief and factual summary of the document indicative of the report, even though it may also appear elsewhere in the body of the technical report. If additional space is required, a continuation sheet shall be attached.

It is highly desirable that the abstract of classified reports be unclassified. Each paragraph of the abstract shall end with an indication of the military security classification of the information in the paragraph, represented as (TS), (S), (C), or (U).

There is no limitation on the length of the abstract. However, the suggested length is from 150 to 225 words.

14. KEY WORDS: Key words are technically meaningful terms or short phrases that characterize a report and may be used as index entries for cataloging the report. Key words must be selected so that no security classification is required. Identifiers, such as equipment model designation, trade name, military project code name, geographic location, may be used as key words but will be followed by an indication of technical context. The assignment of links, rules, and weights is optional.

ER 2391

ANALYTICAL, EXPERIMENTAL AND MECHANICAL
EVALUATION OF FREE ROTATING VANELESS DIFFUSERS

Final Report
Edited By

C. Rodgers

May 1972

Details of illustrations in
this document may be better
studied on microfiche

U. S. Army Mobility Equipment Research and Development Center
Fort Belvoir, Virginia

DA Project 1G663702DG11-01

Contract DAAK02-71-C-0189

Solar Division of International Harvester Company
2200 Pacific Highway, San Diego, California 92112

Distribution of this report is unlimited

ic

SUMMARY

Experimental testing of a model free rotating vaneless diffuser rig to determine diffuser loss coefficients and static pressure recovery under braked and free rotating conditions was conducted. The rig was operated at entry Mach numbers up to unity with both vaned and vaneless diffusers installed downstream. Two rotating diffuser widths wer э tested.

A significant improvement in diffuser performance was achieved under free rotating conditions, even though large wakes generated by upstream stationary swirl nozzles were present. Overall static pressure recovery for the complete diffusion system increased approximately 20%, at free rotating conditions corresponding to a tangential velocity ratio (diffuser/ incident stream) of 0.43. The total pressure loss reduction between braked and rotating conditions correlated with theoretical studies. A mechanical design study to examine methods of integrating the rotating diffuser into a complete gas turbine was also conducted and a feasible preliminary design identified.

ii

FOREWORD

This final technical report covers all theoretical and experimental work necessary to fulfill the requirements of contract DAAK02-71-C-0189 for DA Project 1G6637021D11-01. The contract, authorized by the U.S. Army Mobility Equipment Research and Development Center, Fort Belvoir, Virginia, was awarded to Solar Division of International Harvester Company, 2200 Pacific Highway, San Diego, California on 26 October 1970. The program was conducted by Solar during the period 25 February 1971 to 29 February 1972.

The technical representative of the U.S. Army was Donald Faehn, Project Engineer, Electrotechnology Department, USA MERDC.

The principal investigator responsible for the technical content, execution, and liaison of the program was C. Rodgers. Mr. H. Mnew, Engineering Staff Specialist, was responsible for theoretical and data reduction programs. Other Solar personnel engaged on the program included L. Blinman, Program Manager, J. Thayer, Experimental Engineer, D. Root, Design Engineer.

CONTENTS

Preceding page blank

v/

ILLUSTRATIONS

Preceding page blank vii

ILLUSTRATIONS (Cont)

LIST OF TABLES

SECTION 1

INTRODUCTION

Efficient small radial compressors, with higher pressure ratios and adequate surge margins, are required for future gas turbines. Achieving these requirements necessitates development of newer methods in reducing the energy losses associated with diffusion from supersonic flow conditions, and in increasing the stable operating ranges of diffusion systems between the stalling and choking flow limits. One such method is the replacement of the vaneless diffuser section of a typical high pressure single stage centrifugal compressor by a free rotating vaneless diffuser, within which the relative velocity is subsonic and low loss diffusion can be achieved by virtue of reduced shear forces between the flow and diffuser shrouds.

In order to investigate the feasibility of free rotating diffusers for small centrifugal compressors, an experimental program to design, manufacture, and test a model rotating diffuser was sponsored by U.S. Army MERDC, Reference No. 1. Although this program essentially established the feasibility of the concept, difficulty was experienced in accurately measuring the total pressure loss. This was primarily due to the relatively small pressure levels involved in operating the diffuser at low inlet Mach number conditions with atmospheric discharge pressure, compared with normal instrumentation errors.

1

A continuation program was therefore awarded, by U. S. Army MERDC, to operate the experimental free rotating diffuser model airflow rig up to supersonic inlet Mach numbers in order to increase the pressure levels and thereby minimize the effect of measurement errors. It was further decided to more closely simulate the actual operating environment of a free rotating vaneless diffuser, by incorporating a stationary vaned diffuser downstream of the rotating diffuser. This airflow rig was to be operated to determine rotating diffuser and overall diffuser system loss coefficients and static pressure recoveries, together with braked torques and free rotational speeds. The influence of three-dimensional effects on diffuser performance was to be investigated by testing rotating diffusers with passage widths of 0.35 and 0.23 inch respectively.

To complete the continuation program, a mechanical design study was planned to study various methods of integrating a high pressure ratio centrifugal compressor with a free rotating vaneless diffuser into a complete gas turbine engine assembly. Both manufacturing methods and various ways of supporting the rotating diffuser were to be examined, and a selected preliminary engine layout prepared to define a compressor system suitable for detail design and future rig or engine testing.

SECTION 2

THEORETICAL STUDIES

Performance Prediction

The analysis of the previous test program results (Reference No. 1) was

extended to cover the conditions of the current test program and the range

of potential applications. For this purpose the system of partial differential

and ancillary equations, which describe the compressible flow through

a rotating vaneless diffuser, was reprogrammed for solution using the

IBM system 360 Continuous System Modeling Program (CSMP). This

program is a digital analog simulator, similar to that used previously,

but can accept Fortran statements in addition to the functional analog

"blocks." The simulation is listed in Appendix 2, which corresponds

exactly to the analog schematic, figure 2-4 of Reference No. 1. The

program is oriented to the solution of time variant problems, and

it was necessary to replace time as the independent variable with

diameter ratio $(D/D_2)^*$. More exactly, $(\frac{D}{D_2} - 1)$ corresponds to time

with zero time occurring when $D = D_2$, and increments in diameter ratio

correspond to increments in time. The integration procedure chosen

was the fixed step Runge-Kutta (RKSFX) method, and the integration

step size was chosen from experience to ensure adequate accuracy

without excessive running time.

---

* Stations 2 and 3 refer to diffuser rotor entry and exit in the theoretical
  analysis, whereas these planes are identified by suffixes 3 and 4 in the
  test section.

3

Typical output from the CSMP program is shown in figures 1, 2, and 3, where rotating vaneless diffuser performance parameters are plotted versus inlet Mach number M_2 for a diffuser diameter ratio $D_3/D_2 = 1.3$, and for inlet angles α_2 of 70, 75 and 80 degrees respectively. Theoretical performances at other diameter ratios and inlet flow conditions can be obtained using the CSMP program listed in Appendix 2.

4

SECTION 3

EXPERIMENTAL EQUIPMENT AND PROCEDURE

3.1 TEST RIG DESCRIPTION

A schematic drawing of the test cell layout is shown in figure 4. The operating controls and instrumentation readout devices were located in the control room outside of the test cell. Figure 5 shows the general arrangement of the experimental equipment.

A cross-section of the rotating vaneless diffuser test rig, assembly number 110417, is shown in figure 6. The rig was assembled with either one of two nominal channel widths by incorporating the appropriate rotor and vanes. The -0 assembly had a nominal channel width of 0.350 inch and the -100 assembly had a nominal channel width of 0.230 inch. The rotating vaneless diffuser assembly was composed of a stainless steel main disk and an aluminum outer annular disk. The outer disk was supported from the main disk by seven circular struts of 0.038-inch diameter for the -0 assembly and 0.025-inch diameter for the -100 assembly. A light press fit and epoxy adhesive retained the struts in match drilled holes in both disks.

Sixteen adjustable swirl generating nozzles provided diffuser inlet swirl at angles between 65 and 80 degrees to the radial outflow direction. A major change, incorporated into the rig for this test program, was the addition of fixed channel diffuser vanes at the exit of the rotating vaneless diffuser. These vanes were set at either one of two throat gap settings or, in some instances, were omitted entirely. In this latter case of a vaneless downstream diffuser, small circular spacers were used in the flow path for structural support.

Static pressure taps and fittings for mounting thermocouples and Kiel total-pressure probes were installed in the inlet duct and forward flange assembly, P/N 110338, and in the aft outer flange, P/N 110339. It may be seen in figure 6 that the outer disk of the rotating diffuser was partially enclosed by a sliding ring, P/N 110340, fitted in the forward flange. The sliding ring incorporated two 0.100-inch-diameter holes, one at the rotating diffuser inlet radius, and one at the exit radius. The two holes in the sliding ring enabled the insertion of a total pressure-yaw angle traversing probe into the airstream at selected circumferential positions at the rotating diffuser exit and inlet. A base for mounting and indexing the traversing probe actuator was provided. The four studs of the sliding ring were used to locate and attach the base to the outside of the forward flange. A bracket located directly behind the speed sensing nut of the rotating diffuser support shaft mounted an electromagnetic inductance probe for speed sensing.

6

3.2 INSTRUMENTATION

The test rig instrumentation is listed in Table 1.

Provisions were made for traversing the rotating diffuser inlet and exit for total pressure and yaw angle. A specially fabricated cobra head probe, incorporating a miniature sized head to minimize air blockage in the flow channel, was used for the traverse; see figure 7. The probe was mounted in a subminiature, electronically controlled, L.C. Smith traverse actuator. The probe could be positioned at any desired depth in the channel, or a continuous traverse made. The side ports of the cobra probe were connected to a differential pressure transducer, which in turn was connected to the L.C. Smith Automatic Angle Control. This control sensed any pressure unbalance between the two side ports and automatically controlled the actuator to maintain the pressure balance and keep the probe directed upstream. The resulting yaw angle was fed to the X-Y-Y' plotter. The center, or total, pressure port of the cobra probe was attached to a manometer or to a pressure transducer. The signal from the pressure transducer was amplified in the signal conditioner and then fed to the X-Y-Y' plotter.

Prior to installing the traversing equipment in the test rig, the cobra head probe was individually calibrated for total pressure readout at subsonic and transonic flows in nozzle sections with 0.32- and 0.20-inch openings. The entire traversing system was then calibrated for both total pressure and yaw angle readout and was found to have essentially no error. The installation of the traversing equipment in the air flow rig is shown in figure 5.

7

3.3 METHOD OF TEST

Rig performance runs were made with full instrumentation connected. Testing of the 0.350-inch channel-width assembly was conducted first, followed by testing with the 0.230-inch channel-width assembly. Variations of rotating vaneless diffuser (RVD) aerodynamic conditions were achieved by varying the total to static pressure ratio (P_1/p_4 – inlet duct to RVD exit) and by changing the swirl nozzle throat opening. The rotating diffuser was also tested with and without a downstream channel vaned diffuser and in the braked and free rotating condition. The rotor braking torques were measured with a simple load arm and weights.

For each data point, continuous axial traverses were made at six circumferential positions at both the rotor inlet and exit. A typical axial traverse of the flow angle and total pressure from the cobra probe is shown in figure 8. Oscillation of the angle (yaw) trace was a result of the continuous nulling of the probe around the maximum total pressure point. Physical limitations of the traverse equipment necessitated traversing slightly ahead and aft of the rotor. Traverse station diameters were 5.8 and 8.0 inches compared to rotor ID and OD of 6.0 and 7.8 inches.

The maximum overspeed limit for the 0.350-inch-channel assembly was 22,000 r.p.m., The overspeed limit of the 0.230-inch-channel assembly was 20,000 r.p.m.

8

3.4 TEST CONFIGURATIONS

The various test configurations, operating pressure ratios P_1/p_4, and corresponding data points are listed in Table 2. The 0.35-inch-width rotor was tested with three downstream diffuser configurations; i.e., vaned diffuser throat openings of 0.495 and 0.426 inch and a vaneless diffuser. The 0.23-inch rotor was tested with the vaned diffuser throat opening of 0.495-inch and a vaneless diffuser. The vaned diffuser area ratios (exit/throat) and throat to exit channel lengths for the 0.495 and 0.426 throats were 1.96, 2.22, and 3.8 inches, respectively.

The aerodynamic features of the diffuser rig are shown in figures 9 and 10. Figure 11 shows a comparison of the 0.35- and 0.23-inch-width rotors.

3.5 DATA REDUCTION

Reduction of the test measurements to rotating diffuser performance parameters was conducted on computer program "419 RVD DATA Reduction Program", written in Fortran IV language, and stored for instant access in the IBM 360/50 system.

The program analysis is based on the following instrumentation and procedures:

- Flow measurement by an upstream ASME sharp edged orifice
- Swirl nozzle inlet total pressure and temperature
- Swirl nozzle throat static pressure
- Diffuser rotor inlet wall static pressure
- Diffuser rotor exit wall static pressure

9

- Vaned diffuser throat static pressure

- Vaned diffuser throat total pressure

- Vaned diffuser exit static pressure

- Vaned diffuser exit total pressure

  Vaned diffuser exit total temperature

- Rotational speed

Total pressures and yaw angles from the cobra traverse probe were manually
transcribed from the ¨-Y plotter both at the diffuser rotor inlet and exit for
input into the program 419. Pressures and angles were read at the six
circumferential stations covering one nozzle pitch and the end points (wake to
wake), checked for continuity, and averaged. At each circumferential station,
pressures and angles were read at the centers of five equally spaced axial
rings, which in conjunction with the five circumferential stations formed a
25-point traverse input at the diffuser rotor entry and exit respectively.
For a large part of the testing, the traverse probe was in the nozzle vane
wake making its angle reading of doubtful accuracy; nevertheless, all
measured angles were used for input.

Pressure loss and static pressure recoveries were based upon mass
averaged total pressures and averaged wall static pressures. Measured
flow angles were also mass averaged and used to compute flow blockages
at stations 3 and 4.

All manometer pressure data was recorded twice, once prior and once subsequent to inlet and exit traversing, which required approximately 50 minutes. Data reductions were made for both data sets and subsequently examined to check continuity.

Typical program output for data point 37 is listed in Table 3. Test geometry, rotor speed ratio, airflow, static pressure recoveries, and total pressure loss coefficients are listed prior to tabulation of the vector conditions at each measurement station.

Reduced data for both diffuser rotor widths are listed in Tables 4, 5, and 6.

SECTION 4

DISCUSSION OF RESULTS

Performance testing of the various diffuser configurations was conducted with full instrumentation over the range of conditions shown in Table 2. At each of these conditions (braked and rotating), axial traverses at six equally spaced circumferential positions over one swirl generating nozzle pitch were conducted at the inlet and exit of the model free rotating vaneless diffuser rotor. Traverse station inlet and exit diameters were 5.8 and 8.0 inches respectively, compared to actual rotor inlet and exit diameters of 6.0 and 7.8 inches respectively. In order to compare test results with theoretical predictions, it was necessary to adjust theoretical pressure loss computations to include additional losses over the stationary vaneless space diffusion path between the 5.8- to 6.0-inch-, and 7.8- to 8.0-inch-diameter sections.

4.1 DIFFUSER ROTOR INLET AND EXIT FLOW DISTRIBUTIONS

Stationary swirl nozzle vanes, adjustable to ± 5 degrees of the nominal angle setting, were used to simulate outlet flow conditions representative of a centrifugal compressor impeller. The nozzles were designed as an axial cascade to give the correct outlet angle and then converted to a circular cascade by transformation, Reference No. 1. The minimum number of nozzle vanes, consistent with the solidity requirements for the amount of

Preceding page blank

desired turning, was originally selected to reduce the number of wakes and provide a larger traverse area. Unfortunately, this resulted in a low aspect ratio of 0.25 which proved to be conducive to increased secondary flow losses.

Diffuser inlet absolute Mach number over one swirl nozzle pitch is shown isometrically on figure 12. This distribution was typical of the inlet flow conditions generated by the upstream stationary swirl nozzles for all tests. The core flow is near symmetrical, but separation from the nozzle suction surface aft of the nozzle throat added to the wake from the nozzle trailing edge resulted in a nonuniform shear flow adjacent to the suction surface. The relative position of the separated flow zone in relation to the fixed traverse stations altered with each particular setting of the nozzle throats. Although the pattern was repeatable in general form, a considerable variation in calculated inlet flow blockage B_3 was experienced from 0.05 to 0.20, with an average value of 0.13. For a large part of the testing, the traverse probe at the diffuser rotor inlet was in the swirl nozzle wake, making its angle reading of doubtful accuracy.

The nozzle suction surface separation was substantiated by lampblack flow traces shown on figure 13. Attempts to delay nozzle separation by increasing turbulence with a close mesh screen forward of the nozzle leading edge did not materially change the exit flow distribution. Rather than attempt a nozzle redesign to provide improved diffuser rotor entry flow conditions, it was considered judicious, at that time, to continue diffuser performance evaluation testing.

14

This type of spiral vortex flow, with the time-steady wakes from the nozzle vanes and zones of time-steady separation, is not representative of the flow at the discharge of an actual centrifugal compressor impeller where rapid mixing takes place. It is for this reason that caution is necessary in interpretation of the results in terms of absolute loss level and absolute static pressure recoveries.

Axial and circumferential variations of diffuser rotor inlet and exit absolute Mach numbers for selected data points are shown in figures 14 thru 18 in terms of local to mass averaged values of M_3 and M_4. Braked and free-rotating traverse plots are shown on each separate figure for comparison. Examination of these Mach number ratio plots reveals the type of inlet flow previously discussed, with the swirl nozzle wake affecting flow symmetry. The wake appears to propagate to the diffuser rotor exit, but diminishes in strength, whereas the main throughflow at the exit tends to migrate toward the aft shroud. This migration diminishes under free rotating conditions, which together with a reduced variation of exit Mach number ratio M_4/M_4 average indicates a general flow smoothing effect. Attempts were made to obtain diffuser rotor shroud boundary layer flow patterns by the injection of oil, followed by lampblack, into the flow system. The intent was to show the shorter relative streamline path, compared to the longer spiral vortex path in the main core flow. Various proportions of oil and lampblack were tried, but all were unsuccessful due to centrifuging of the wall oil films in an almost radially outward direction.

15

The diffuser rotor inlet profiles were essentially similar with both the 0.35- and 0.23-inch width rotors except that the nozzle losses increased (see Section 4.2.2) with the smaller width rotor due to a reduction in aspect ratio from 0.25 to 0.16.

At the termination of the test program, the chord of the swirl nozzle was reduced from 1.33 to 0.90 inches, by grinding away the leading edge in an attempt to improve the diffuser entry flow distribution, and by increase of the nozzle aspect ratio. Tests with the modified nozzle showed essentially the same diffuser performance as previously measured for data points 21 to 28. It is considered, therefore, that either an increase in nozzle vane number or decrease in suction surface back curvature would be required to improve the diffuser entry flow conditions.

4.2 DIFFUSER TEST PERFORMANCES

4.2.1 0.35-Inch-Width Rotor

The 0.35-inch-width free rotating vaneless diffuser was flow tested with two vaned diffuser configurations and a vaneless diffuser downstream of the rotor. Diffuser performance both across the rotor and over the complete diffusion system is shown on figure 19 for a vaned diffuser throat opening of 0.495 inch and the vaneless diffuser. Static pressure recoveries, total pressure loss coefficients, air angles, and Mach numbers are shown plotted against an abscissa of diffuser rotor inlet flow function $W\sqrt{T_3}/P_3$. Selection of the inlet flow function as a correlating performance parameter rather than inlet flow angle was made to avoid data scatter from the

16

measured flow angle. It can be shown that for Mach numbers in the range 0.8 to 1.1, the flow angle (fixed annulus geometry) is proportioned to $W\sqrt{T_3}/P_3$. The data shown on figure 19 was obtained with two settings of the swirl generating nozzles ($O_t = 0.38$ and 0.31 inch). Of primary significance is an increase in peak overall static pressure recovery $C_{p\ 3-6}$ from 0.54 braked to 0.66 free rotating, amounting to a 22% increase in static pressure recovery. Figure 20 shows the estimated influence of diffuser static pressure recovery on efficiencies of typical high pressure ratio single stage centrifugal compressors. A 22% increase in C_p would provide an increase in overall efficiency of between 4 and 5% points.

Performance data with the second vaned diffuser (O_D 0.426-inch) and a vaneless diffuser downstream is shown on figure 21. Peak overall static pressure recovery increases from 0.52 braked to 0.64 free rotating, again amounting to a substantial 22% increase in static pressure recovery. Rotor performance $C_{p\ 3-4}$ and $\Delta P_{3-4}/q_3$ is essentially independent of the downstream diffuser configuration (i.e. vaned or vaneless).

Total pressure loss coefficients, both braked and free rotating across the rotor, $\Delta P_{3-4}/q_3$, are shown plotted against rotor inlet Mach number M_3 on figure 22 for all test conditions with the 0.35-inch-width rotor. The difference in loss coefficient between braked and free rotating operation correlates closely with the theoretical studies as is discussed later.

The characteristics of the swirl generating nozzles employed with the 0.35-inch-width rotor are shown in figure 23. Increase in exit Mach number results in a considerable increase in nozzle loss coefficient, probably

due to the diffusion process commencing from the nozzle throat outwards, requiring supersonic conditions ($M_2 > 1.05$) at the nozzle throat to reach sonic conditions at the rotor entry. The relatively low static pressure recovery of 0.54 under braked conditions is entirely due to the poor flow distribution generated by the stationary swirl nozzles ($B_{3\ avg} = 0.13$) and is typical of the results obtained by Wolf and Johnston, Reference No. 2, for diffusers with nonuniform inlet velocity profiles.. Considerably smoother flow is generated by high performance centrifugal compressors which additionally create rapid mixing due to high rotational speeds. Static pressure recoveries of 0.70 have been measured for similar channel diffusers operating up to entry Mach numbers of unity on Solar centrifugal compressor rigs.

The decrease in overall static pressure recovery with increasing inlet flow, shown on figure 19, is a consequence of approaching stationary vaned diffuser choke. Choke data was obtained with a swirl nozzle throat opening O_t of 0.380 inch. In order to determine diffuser performance close to stall, the swirl nozzle throat opening was reduced to 0.310 inch. No clear evidence of stall was apparent at the reduced flows, although it does appear that both the overall static pressure recovery and loss coefficient are approaching their maximum and minimum levels.

4.2.3 0.23-Inch-Width Rotor

The 0.23-inch-width free rotating vaneless diffuser was flow tested with one vaned diffuser configuration and a vaneless diffuser downstream of the rotor.

18

Diffuser performance both across the rotor and over the complete diffusion system, is shown on figure 24. Peak overall static pressure recovery increases from 0.49 braked to 0.6 free rotating, providing the same percentage increase (22%) in static pressure recovery as the 0.35-inch rotor.

Total pressure loss coefficients, both braked and free rotating, $\Delta P_{3-4}/q3$, are shown plotted versus rotor inlet Mach numbers M_3 on figure 25. Swirl generating nozzle flow characteristics for the 0.23-inch rotor are shown on figure 26.

4.3 FREE ROTATING SPEEDS

Free rotating speeds (r.p.m.) and speed ratios U_3/C_{U3} for the two rotor widths tested are shown plotted on figure 27 versus inlet Mach number M_3. The speed ratio U_3/C_{U3} remained essentially constant at 0.43 over the range of operating conditions for both rotating diffuser widths, indicating the effect of passage width on the wall shear forces was small.

It was calculated that the increase in friction coefficient for the smaller width rotor would be approximately 9%, and that the U_3/C_{U3} at free rotating conditions (with the same parasitic resisting drag characteristic) would therefore increase approximately 2%. Further reductions in passage width would of course finally result in encroachment of the two shroud boundary layers with a resulting Couette type flow.

4.4 FRICTION COEFFICIENTS

Theoretical performance predictions for vaneless diffuser systems were completed assuming a constant friction coefficient C_f of 0.005. It was possible to experimentally determine friction coefficients for the model airflow rig using two methods discussed as follows:

4.4.1 Braked Torque Method

Diffuser net torque under braked ($U_3/C_{U3} = 0$) conditions was measured using a simple load arm. The torques measured under these conditions are listed in Tables 4, 5, and 6, and include the drag of the small diameter supporting struts. Separating out the st ut drag (turbulent flow conditions $C_D = 1.0$), it was possible to determine the torque generated by frictional shear along both shrouds of the diffuser and to thereby calculate the friction coefficient using the expression:

$$\overline{C}_f = \frac{2 \, b \, \text{Torque} \cos \left(\frac{a3 + a4}{2} \right)}{\frac{W}{g} \left(r_3 C_{U3} + r_4 C_{U4} \right) \left(r_4 - r_3 \right)}$$

Where $\overline{C}_f$ = friction coefficient based on mass averaged core flow conditions.

4.4.2 Traverse Probe as Preston Tube

The Preston tube technique, Reference No. 3, is a convenient method for measurement of wall shear stress over smooth boundaries. The technique involves the use of a small calibrated probe placed on the wall to measure stagnation pressure. Reference No. 4 suggested the use of a yaw probe as Preston tube, and Reference No. 5 gives a simplified method of calculating

20

the local (wall) friction coefficient C_f from Preston tube data. The method used herein was to use the traverse probe stagnation pressures at the shroud, the shroud static pressure, core flow velocity, and the probe diameter to calculate C_f at the inlet to the diffuser rotor.

4.4.3 Comparision of Test Friction Coefficients

Both $\bar{C}_f$ core and C_f wall calculated from braked torque and traverse probe readings (clear of the swirl nozzle wake) are compared on figure 28 against an abscissa of core flow Reynolds number defined as:

$$R_e = \frac{b}{2} \frac{(C_3 + C_4)/2}{\nu}$$

Relatively good agreement of both experimentally derived friction coefficients with the relationship $C_f = 0.046 \, R_e^{-0.2}$ is apparent.

4.5 COMPARISON OF TEST AND THEORETICAL PERFORMANCES

As mentioned previously, the distorted flow from the stationary swirl nozzles makes comparison of the theoretical and test performances of the free rotating diffuser difficult. The theoretical model (Appendix 2) assumed the only loss source was that incurred in frictional resistance along the diffuser shrouds. Pressure losses in the experimental model with the distorted entry flow comprise frictional resistance, mixing, and secondary flow losses. Under these conditions, it was only possible to achieve a complete diffusion system braked static pressure recovery of 0.54 with an average inlet blockage factor, B_3, of 0.13, for the 0.35-inch-width rotor.

Higher static pressure recoveries (up to 0.70 at Solar) are attainable with cleaner mixed flow from well designed centrifugal compressor components. The minimum braked loss coefficient across the 0.35-inch-width rotor for an inlet angle, α_3, of 70 degrees and Mach number of 0.95 was 0.243 compared to a theoretically predicted value of 0.08. This large difference in absolute loss coefficient is attributed to loss sources (secondary, mixing, etc.) other than friction.

Further examination of the test data, however, did reveal a consistent correlation of theoretical and test results when the loss difference $\Delta P_{3-4}/q_3$ [braked - rotating] was compared.

The theoretical performance program described in Appendix 2 was used to predict the loss difference for the experimental model diffuser and included those additional friction losses along the stationary sections of the flow path between stations 3 and 4 necessary for traversing. Theoretically predicted model diffuser performance is shown on figure 29 for a range of inlet Mach numbers and inlet flow angles. Data from figure 29 is compared to actual test loss differences at various operating conditions in Table 7. This comparison reveals close agreement and leads to the conclusion that the measured loss difference is that basically arising from reduction in frictional losses. This is substantiated by two other independent measurements, for in order to obtain such an agreement between measured and theoretical friction loss, the test friction loss coefficient C_f should be close to that assumed ($Cf = 0.005$) in the analytical model. The plot of test friction coefficients (figure 28) from both braked

22

torque measurements, and use of the traverse probe as a Preston tube, do indeed independently substantiate the measured loss differences from the traverse data.

Summarizing, the experiments have demonstrated the substantial reduction in friction loss that can be obtained in vaneless diffusers by rotating the sidewalls. The absolute performance level of any diffusion system (either stationary or rotating) will always be dependent upon the inlet flow profile, cleaner flows leading to higher performances.

In these particular exploratory experiments, it was considered prudent to start with a simulated inlet flow condition rather than immediate evaluation on an actual compressor rig. It is now evident that the simulated flow was quite different in nature to that discharging from a high speed rotating impeller; nevertheless, the experiments have demonstrated the theoretical performance predictions, and the next phase in the development of the supersonic diffusion concept should involve actual performance evaluation in a compressor test rig.

SECTION 5

CONCLUSIONS

* Theoretical studies, corroborated by experiments, have shown that frictional losses in vaneless diffusers for centrifugal compressors can be reduced by 70% by allowing the diffuser to rotate at tangential speed ratios (rotor/incident stream) above 0.4.

* Overall static pressure recovery for a vaneless diffuser of diameter ratio 1.3, followed by a vaned diffuser system, can be increased 22% by rotating the vaneless section at speed ratios above 0.4.

* It is estimated that an increase in overall compressor efficiency of between 4 and 5% points could be obtained by installing a free rotating vaneless diffuser in an advanced high pressure ratio single stage centrifugal compressor.

* Free rotating diffusers do tend to smooth out distorted entry flow profiles, thereby inducing increased flow ranges and higher performances for downstream diffusion systems.

* Tests on two rotors with passage widths of 0.35 and 0.23 inch revealed no significant three dimensional effects on the reduction in frictional losses from braked to free rotating conditions. Free rotating speed ratios U_3/C_{U3} were essentially the same for both diffuser rotors at constant incident flow conditions.

- An application design study was completed, establishing that the concept of integrating a free rotating vaneless diffuser in an advanced 100 kW gas turbine is feasible and will provide performance improvements at the the expense of increased cost and complexity.

SECTION 6

RECOMMENDATIONS

- Development of the free rotating vaneless diffuser should be continued to the stage of evaluating its performance in an actual high-pressure-ratio centrifugal-compressor rig.

- The rotating diffuser configuration recommended for compressor test rig evaluation is an integrally machined assembly with fifteen (or more) airfoil-shaped "neutral" front-shroud-supporting vanes.

- Due to the complex mechanical structural configuration of the free rotating diffuser and the relatively high tip speeds at which the cantilevered assembly operates, a mechanical test program should be conducted to determine distortions, burst speed, etc., prior to aerodynamic testing.

SECTION 7

GLOSSARY

B	Boundary layer blockage $= 1 - \dfrac{\text{Effective area}}{\text{Geometrical area}}$	
b	Blade height	inch/ft
C	Velocity	f.p.s.
C_p	Static pressure recovery (based on mass averaged dynamic head)	
C_f	Local skin friction coefficient	
$\overline{C}_f$	Skin friction coefficient based on core flow	
D	Diameter	inch
G	Gravitational constant	ft./sec.^{2}
L	Length	inch
M	Mach number	
N	Rotational speed	r.p.m.
O_t	Swirl nozzle throat opening	inch
O_D	Vaned diffuser throat opening	inch
P	Total pressure	p.s.i.a.
p	Static pressure	p.s.i.a.
q	Dynamic pressure	p.s.i.a.
r	Radius	inch
T	Total temperature	°R
t	Static temperature	°R
U	Tangential speed	f.p.s.
W	Airflow	lb./sec.

GREEK

α	Streamline angle	degree
β	Blade angle	degree
ν	Kinematic viscosity	lb.-ft./sec.^{2}
Δ	Difference	
η	Efficiency	%
ρ	Density	lb./ft.^{3}

SUBSCRIPTS

1	Swirl nozzle or compressor inlet
2	Swirl nozzle or compressor exit
3	Rotating diffuser inlet
4	Rotating diffuser exit
5	Vaned diffuser inlet
6	Vaned diffuser exit
C	Compressor
U	Tangential direction

NOTE: Stations 3 and 4 refer to diffuser rotor entry and exit in the test program section, whereas these planes are identified by suffixes 2 and 3 in the theoretical analysis reference Appendix 2.

30

SECTION 8

REFERENCES

1. C. Rodgers, H. Mnew, Rotating Vaneless Diffuser Study
    October 1970, USA, MERDC, AD 716370

2. S. Wolf, J. P. Johnston, Effects of Nonuniform Inlet Velocity
    Profiles on Flow Regimes and Regimes
    in Two Dimensional Diffusers
    A.S.M.E. 68 – WA/FE-25.

3. E. J. Hopkins, E. R. Keener, Study of Surface Pitots for Measuring
    Turbulent Skin Friction of Supersonic
    Mach Numbers – Adiabatic Wall
    NASA TN D 3478, July 1966.

4. N. Rojaratnam, D. Muralidhar, Yaw Probe Used as Preston Tube
    R.AeS Quarterly, December 1968.

5. M. R. Head, V. Vasanta Ram, Simplified Presentation of Preston
    Tube Calibration, R.AeS Quarterly,
    August 1971.

TABLE 1

ROTATING VANELESS DIFFUSER RIG INSTRUMENTATION LIST

CODE	LOCATION	MEASUREMENT	SENSOR TYPE	QTY	ESTIMATED RANGE	READOUT DEVICE	MEASUREMENT SYSTEM ABSOLUTE UNCERTAINTY	CONFIDENCE LEVEL	REMARKS
P_{T1}	Inlet duct (Station 1)	Total pressure	Kiel probe	1	0 to 21"Hg	Manometer	±.05"Hg	95%	
T_1, T_2, T_3		Total temperature	T/C half shielded T/C	3	55 to 100°F	Self balancing potentiometer	±8°F	95%	
P_2, P_3, P_4, P_5	Swirl nozzle throat (Station 2)	Static pressure	Wall tap	4	-14 to 0"Hg	Manometer	±.05"Hg	95%	Read 3 per data point
$P_6, P_7, P_8, P_9, P_{10}, P_{11}$	RVD Inlet (Station 3)	Static pressure	Wall tap	6	-14 to 0"Hg	Manometer	±.05"Hg	95%	Read 5 per data point
$P_{12}, P_{13}, P_{14}, P_{15}, P_{16}, P_{17}$	RVD Exit (Station 4)	Static pressure	Wall tap	6	-10 to 0"Hg	Manometer	±.05"Hg	95%	Read 5 per data point
$P_{18}, P_{19}, P_{20}, P_{21}$	Vaned diffuser throat (Station 5)	Static pressure	Wall tap	4	-10 to 0"Hg	Manometer	±.05"Hg	95%	
P_{T44}		Total pressure	Kiel probe	1	0-10"Hg	Manometer	±.05"Hg	95%	Installed after P19
P_{22}, P_{23}, P_{24}	Vaned diffuser exit (Station 6)	Static pressure	Wall tap	3	-5 to 0"H$_2$O	Manometer	±.05"H$_2$O	95%	
$P_{T25}, P_{T26}, P_{T27}, P_{T28}$		Total pressure	Total press rake	4	0 to 21"Hg	Manometer	±.05"Hg	95%	
T_4, T_5, T_6		Total temp	T/C half shielded T/C	3	55 to 100°F	Self balancing potentiometer	±8°F	95%	
$P_{T29}, P_{T30}, P_{T31}, P_{T32}, P_{T33}, P_{T34}$	RVD Inlet (Station 3)	Total pressure	Cobra probe	1	-5 to 10 psig	Pressure transducer to X-Y-Y' plotter	±.07 psig	95%	$P_{T29}-P_{T40}$ and α29-40 will be obtained by consecutively traversing at the P_6-P_{17} locations respectively
α29, α30, α31, α32, α33, α34		Airstream flow direction			65°-105° from radial	X-Y-Y' plotter	±.5 degrees	95%	
$P_{T35}, P_{T36}, P_{T37}, P_{T38}, P_{T39}, P_{T40}$	RVD Exit (Station 4)	Total pressure			-5 to 10 psig	Pressure transducer to X-Y-Y' plotter	±.07 psig	95%	
α35, α36, α37, α38, α39, α40		Airstream flow direction			65°-105° from radial	X-Y-Y' plotter	±.5 degrees	95%	

Preceding page blank

TABLE 1

ROTATING VANELESS DIFFUSER RIG INSTRUMENTATION LIST (Continued)

CODE	LOCATION	MEASUREMENT	SENSOR TYPE	QTY	ESTIMATED RANGE	READ OUT DEVICE	MEASUREMENT SYSTEM ABSOLUTE UNCERTAINTY	CONFIDENCE LEVEL	REMARKS
T_7	Orifice inlet	Total temperature	T/C half shielded T/C	1	55-100°F	Sel. balancing potentiometer	±3°F	95%	
P_{41}		Static pressure	Flange tap manifold	1	0 to 15 psig	Bourdon test gage	±.25 psig	95%	Hg used after DP #9
ΔP_0	Orifice	Static pressure drop across orifice	Flange tap manifolds	2	0-100"H$_2$O or 0-15"Hg	Manometer	±.05"H$_2$O ±.05"Hg	95%	
P_{42}	Labyrinth seal buffer air	Static pressure	Static tap	1	10-20"Hg	Manometer	±.05"Hg	95%	
P_{43}	Bearing oil inlet	Static pressure	Static tap	1	5.to.25 psig	Bourdon gage	±.5 psig	95%	
T_8	Bearing oil inlet	Temperature	T/C shielded ungrounded thermocouple	1	70-90°F	Self balancing potentiometer	±8°F	95%	
T_9	Bearing oil discharge	Temperature	T/C shielded ungrounded thermocouple	1	30-100°F	Self balancing potentiometer	±8°F	95%	
G_1	Bearing housing	Radial vibration	Accelero-meter	1	0-10 G's	Charge amplifier to meter calibrated in G's	±.5 G	95%	
G_2	Aft outer flange	Axial vibration	Accelero-meter	1	0-10 G's	Charge amplifier to meter calibrated in G's	±.5 G	95%	
N	Rotor	Rotor speed	Electro-magnetic inductance probe	1	0-2200 cps	Electronic digital counter	±3.2 cps	95%	

TABLE 2. TEST CONFIGURATIONS

DATA POINT	ROTOR WIDTH INCH	NOMINAL $\frac{U_3}{CU_3}$	SWIRL NOZZLE O_t INCH	VANED DIFFUSER O_D INCH	PRESSURE RATIO P_1/P_4
1	0.35	0	0.380	VANELESS	1.5
2	0.35	0	0.380	VANELESS	1.66
6	0.35	0	0.380	VANELESS	1.4
7	0.35	0.47	0.380	VANELESS	1.5
8	0.35	0.47	0.380	VANELESS	1.66
10	0.35	0	0.380	0.495	1.3
11	0.35	0	0.380	0.495	1.4
12	0.35	0	0.380	0.495	1.5
13	0.35	0	0.380	0.495	1.66
14	0.35	0.44	0.380	0.495	1.3
15	0.35	0.44	0.380	0.495	1.4
16	0.35	0.44	0.380	0.495	1.5
17	0.35	0.44	0.380	0.495	1.66
21	0.35	0	0.310	0.495	1.3
22	0.35	0	0.310	0.495	1.4
23	0.35	0	0.310	0.495	1.5
24	0.35	0	0.310	0.495	1.66
25	0.35	0.42	0.310	0.495	1.3
26	0.35	0.42	0.310	0.495	1.4
27	0.35	0.43	0.310	0.495	1.5
28	0.35	0.43	0.310	0.495	1.66
30	0.35	0	0.267	0.426	1.3
31	0.35	0	0.267	0.426	1.5
32	0.35	0	0.267	0.426	1.7
33	0.35	0	0.267	0.426	1.8
34	0.35	0.42	0.267	0.426	1.3
35	0.35	0.42	0.267	0.426	1.5
36	0.35	0.42	0.267	0 426	1.7
37	0.35	0.45	0.267	0.426	1.8
38	0.35	0	0.267	VANELESS	1.3
39	0.35	0	0.267	VANELESS	1.5
40	0.35	0	0.267	VANELESS	1.7
41	0.35	0.41	0.267	VANELESS	1.3
42	0.35	0.43	0.267	VANELESS	1.5
43	0.35	0.43	0.267	VANELESS	1.7
44	0.23	0	0.310	0.495	1.3
45	0.23	0	0.310	0.495	1.5
46	0.23	0	0.310	0.495	1.7
47	0.23	0	0.310	0.495	1.8
48	0.23	0.42	0.310	0.495	1.3
49	0.23	0.43	0.310	0.495	1.5
50	0.23	0.40	0.310	0.495	1.7
51	0.23	0.44	0.310	0.495	1.8
52	0.23	0	0.429	VANELESS	1.3
53	0.23	0	0.429	VANELESS	1.5
56	0.23	0.43	0.429	VANELESS	1.3
57	0.23	0.43	0.429	VANELESS	1.5

TABLE 3

P-419 RVD DATA REDUCTION PROGRAM

```
              ROTATING VANELESS DIFFUSER, BLD 2C, SNG .267, DVG .426,CELL 30/5
DATA POINT                                           37
NOZZLE THROAT                                       0.3668   IN
VANED DIF THROAT                                    0.4260   IN
VANED DIF EXIT WIDTH                                0.9670   IN
SPEED                                               16600    RPM
MASS FLOW                                           0.6803   PPS
SPEED RATIO (U3/CU3)                                0.4463

RVD               CP(3-4)............     ·        0.2801
VANED DIF         CP(4-6)............              0.6100
VANED DIF         CP(5-6)............              0.5078
O/ALL DIF         CP(3-6)............              0.5837
RVD               DELP(3-4)/Q3........            0.2222
VANED DIF         DELP(4-6)/Q4........            0.2145
VANED DIF         DELP(5-6)/Q5........            0.2774
O/ALL DIF         DELP(3-6)/Q3........            0.3239
NOZZ&VANELESS SPACE DELP(1-3)/Q3..               0.4194

CONDITION AT ST 3   AL3M= 70.28  AL3TH 73.94  CR3= 337.47  CU3= 941.37
CONDITION AT ST 4   AL4M= 77.31  AL4TH 77.06  CR4= 155.30  CU4= 639.80
```

STATION	ST1	ST2	ST3	ST4	ST5	ST6
DIAMETER,IN	2.6890	----	5.0000	8.0000	----	----
CHAN WIDTH,IN	0.6722	0.3200	0.3200	0.3600	0.3610	0.3610
GEO AREA SQIN	5.6786	1.3660	5.0308	9.0478	2.3065	2.5345
BLOCKAGE FACT	1.0000	0.9950	0.8196	1.0195	0.9388	0.8332
FLO AREA,SQIN	5.6786	1.3592	4.6127	2.0260	2.1656	4.3530
FLO PARAM	0.1268	0.5306	0.5312	0.4701	0.4384	0.2307
MACH NO	0.1356	1.0503	0.9689	0.6550	0.5803	0.2615
PT/PS	1.0137	2.0089	1.9259	1.3333	1.2562	1.0487
TT/TS	1.0039	.2203	1.1875	1.0857	1.0673	1.0137
PT PSIA	21.6810	6.6496	18.2242	16.3929	16.4430	15.5120
PS PSIA	21.3878	10.7767	9.9812	12.2902	13.0897	14.7927
TT R	526.7000	525.7000	525.7000	526.7000	526.7000	525.7000
TS R	524.6565	431.6082	443.5420	495.1289	493.5054	510.6015
VELOCITY FPS	156.7630	1069.3843	1000.0342	707.0632	631.8240	292.1768

```
     PROBE DEPTHS OF IMMERSION
STATION 3         .032   0.096   0.160   0.224   0.288
STATION 4         -.0    0.036   0.108   0.180   0.252

     PROBE DEPTHS OF IMMERSION
STATION 3         0.324   0.0
```

TABLE 4

ROTATING VANELESS DIFFUSER TEST DATA TABULATION, ROTOR WIDTH 0.35 INCH

DATA POINT NUMBER	MACH No. M_3	MACH No. M_4	$\frac{W\sqrt{T_3}}{P_3}$	$C_{P_{3-4}}$	$C_{P_{3-6}}$	$\frac{\Delta P_{3-4}}{q_3}$	$\frac{\Delta P_{3-6}}{q_3}$	$\frac{U_3}{CU_3}$	α_{3_M}	α_{4_M}	N r.p.m	STALL TORQUE lb.-ft.	AIRFLOW lb./sec.
1	.8973	.561	1.12	.2960	.465	.2871	.4622	0	64.6	72.0	0	.345	.895
2	.8927	.5638	1.125	.2862	.4597	.2897	.4561	0	64.6	72.0	0	.345	.898
6	.9780	.5961	1.193	.2968	.4604	.3012	.4700	0	63.5	71.3	0	.396	.985
7	.9157	.6219	1.535	.3180	.5107	.2258	.4036	.4737	65.1	73.0	15790	---	.885
8	1.002	.6468	1.203	.3288	.5053	.2029	.3885	.4733	63.6	71.4	17750	---	.969
10	.735	.4945	1.027	.3035	.4132	.2203	.4363	0	67.2	74.4	0	.261	.785
11	.791	.5334	1.049	.2867	.4296	.2337	.4530	0	67.0	74.8	0	.292	.835
12	.873	.5841	1.074	.2920	.4301	.2345	.4481	0	66.8	75.1	0	.350	.878
13	.9567	.5353	1.136	.2780	.3258	.2454	.5533	0	63.8	75.2	0	.418	1.038
14	.8356	.5662	1.069	.3268	.5502	.1825	.3231	.435	66.3	76.1	13940	---	.826
15	.8811	.5926	1.079	.3125	.5442	.1958	.3338	.436	66.3	74.9	14600	---	.841
16	.9245	.6219	1.111	.3112	.5183	.1920	.3516	.443	68.3	76.2	15780	---	.891
17	1.056	.6493	1.120	.2968	.3756	.2874	.4821	.443	68.4	75.1	17750	---	1.045
21	.6315	.4594	.840	.2910	.5543	.2366	.3536	0	68.4	71.8	0	.229	.597
22	.7678	.5161	.880	.2906	.5653	.2339	.3476	0	67.5	74.7	0	.281	.648
23	.8487	.5898	.901	.2887	.5610	.2326	.3513	0	68.1	75.7	0	.317	.685
24	.9497	.6477	.920	.2570	.5142	.2453	.4080	0	67.9	78.5	0	.364	.747
25	.6876	.4870	.844	.3239	.6477	.1455	.2776	.4161	71.5	79.	11600	---	.597
26	.7953	.5581	.880	.3246	.6594	.1437	.2808	.422	72.2	80.0	13430	---	.639
27	.8529	.626	.897	.2885	.6520	.1278	.2844	.4311	71.0	80.7	14430	---	.660
28	.9412	.668	.932	.2789	.6196	.1708	.3108	.434	71.5	79.8	15850	---	.714

TABLE 5
ROTATING VANELESS DIFFUSER TEST DATA TABULATION, ROTOR WIDTH 0.35 INCH

DATA POINT NUMBER	MACH No. M_3	MACH No. M_4	$\dfrac{W\sqrt{T_3}}{P_3}$	$C_{P_{3-4}}$	$C_{P_{3-6}}$	$\dfrac{\Delta P_{3-4}}{q_3}$	$\dfrac{\Delta P_{3-6}}{q_3}$	$\dfrac{U_3}{CU_3}$	α_{3_M}	α_{4_M}	N r.p.m	STALL TORQUE lb.-ft.	AIRFLOW lb./sec.
30	.669	.441	.716	.2874	.5184	.2647	.3859	0	72.7	76.8	0	.213	.5273
31	.858	.556	.780	.2764	.5170	.2806	.3980	0	71.6	77.3	0	.312	.6142
32	.901	.627	.803	.2444	.4804	.3089	.4436	0	71.5	77.8	0	.370	.6758
33	.978	.642	.846	.2475	.4600	.2954	.4605	0	70.1	77.6	0	.390	.7225
34	.833	.702	.742	.3258	.6304	.2180	.2902	.417	72.5	77.7	11860		.5355
35	.892	.605	.771	.3094	.6111	.1965	.3199	.424	71.1	78.9	14700(?)		.5924
36	.981	.665	.814	.2754	.5884	.2239	.3364	.423	70.4	78.2	15860		.6492
37	.962	.645	.845	.2798	.5785	.2247	.3325	.448	70.3	77.3	16770		.6674
38	.671	.425	.723	.2997	.4667	.2851	.4505	0	72.9	76.2	0	.223	.532
39	.851	.552	.777	.2533	.4153	.3085	.5067	0	72.9	77.0	0	.312	.6239
40	.928	.603	.820	.2399	.4049	.3194	.5290	0	70.8	77.0	0	.370	.6881
41	.713	.465	.727	.3246	.4917	.2274	.4369	.408	73.7	78.3	11880		.5469
42	.872	.578	.769	.3060	.4690	.2206	.4633	.425	72.2	77.9	14850		.6163
43	.974	.656	.813	.2740	.4468	.2336	.4850	.433	71.9	78.9	16650		.6852
44	.645	.393	.530	.2803	.4875	.3409	.4136	0	68.5	75.2	0	.177	.389

TABLE 6

ROTATING VANELESS DIFFUSER TEST DATA TABULATION, ROTOR WIDTH 0.23 INCH

DATA POINT NUMBER	MACH No. M_3	MACH No. M_j	$\dfrac{W\sqrt{T_3}}{P_3}$	$C_{P_{3-4}}$	$C_{P_{3-6}}$	$\dfrac{\Delta P_{5-4}}{q_3}$	$\dfrac{\Delta P_{3-6}}{q_3}$	$\dfrac{U_3}{C_{U_3}}$	α_{3_M}	α_{4_M}	N r.p.m.	STALL TORQUE lb.-ft.	AIRFLOW lb./sec.
44	.645	.393	.530	.2803	.4875	.3408	.4136	0	68.5	75.2	0	.177	.389
45	.824	.488	.573	.2683	.4773	.3648	.4353	0	68.4	75.9	0	.261	.455
46	.929	.556	.610	.2562	.4617	.3660	.4418	0	68.3	75.6	0	.318	.5129
47	.983	.565	.625	.2751	.4395	.3740	.4652	0	70.5	74.5	0	.333	.5432
48	.671	.447	.536	.3141	.5941	.2250	.3027	.423	68.8	77.1	11270	---	.3874
49	.848	.552	.560	.300	.5788	.2651	.3287	.430	68.3	77.9	14070	---	.4303
50	.934	.599	.615	.3090	.5503	.2537	.3393	.451	69.1	77.2	16300	---	.4885
51	.981	.615	.651	.3204	.5500	.2550	.3555	.439	71.3	76.3	16640	---	.5274
52	.673	.444	.722	.2820	.4444	.2700	.4693	0	62.3	69.3	0	.197	.5454
53	.880	.553	.776	.3000	.4461	.2803	.4883	0	63.5	70.4	0	.284	.6313
56	.709	.464	.724	.3273	.5020	.2211	.4115	.425	63.4	71.1	11500	---	.5371
57	.898	.571	.769	.3143	.4801	.2470	.4463	.434	64.5	72.2	14700	---	.6157

TABLE 7

COMPARISON OF THEORETICAL AND TEST PERFORMANCES

ROTOR WIDTH INCH	AIR ANGLE a_3 DEG	MACH NUMBER M_3	LOSS DIFFERENCE $\Delta P_{3-4}/q_3$ [Braked–Rotating]	
			Theory	Test
0.35	67	0.8	0.052	0.045
0.35	67	0.9	0.057	0.047
0.35	67	1.0	0.062	0.050
0.35	70	0.8	0.062	0.082
0.35	70	0.9	0.067	0.082
0.35	70	1.0	0.072	0.082
0.35	72	0.8	0.068	0.076
0.35	72	0.9	0.075	0.080
0.35	72	1.0	0.082	0.084
0.23	69	0.8	0.060	0.110
0.23	69	0.9	0.065	0.112
0.23	69	1.0	0.070	0.115
0.23	63	0.8	0.040	0.048
0.23	63	0.9	0.042	0.051
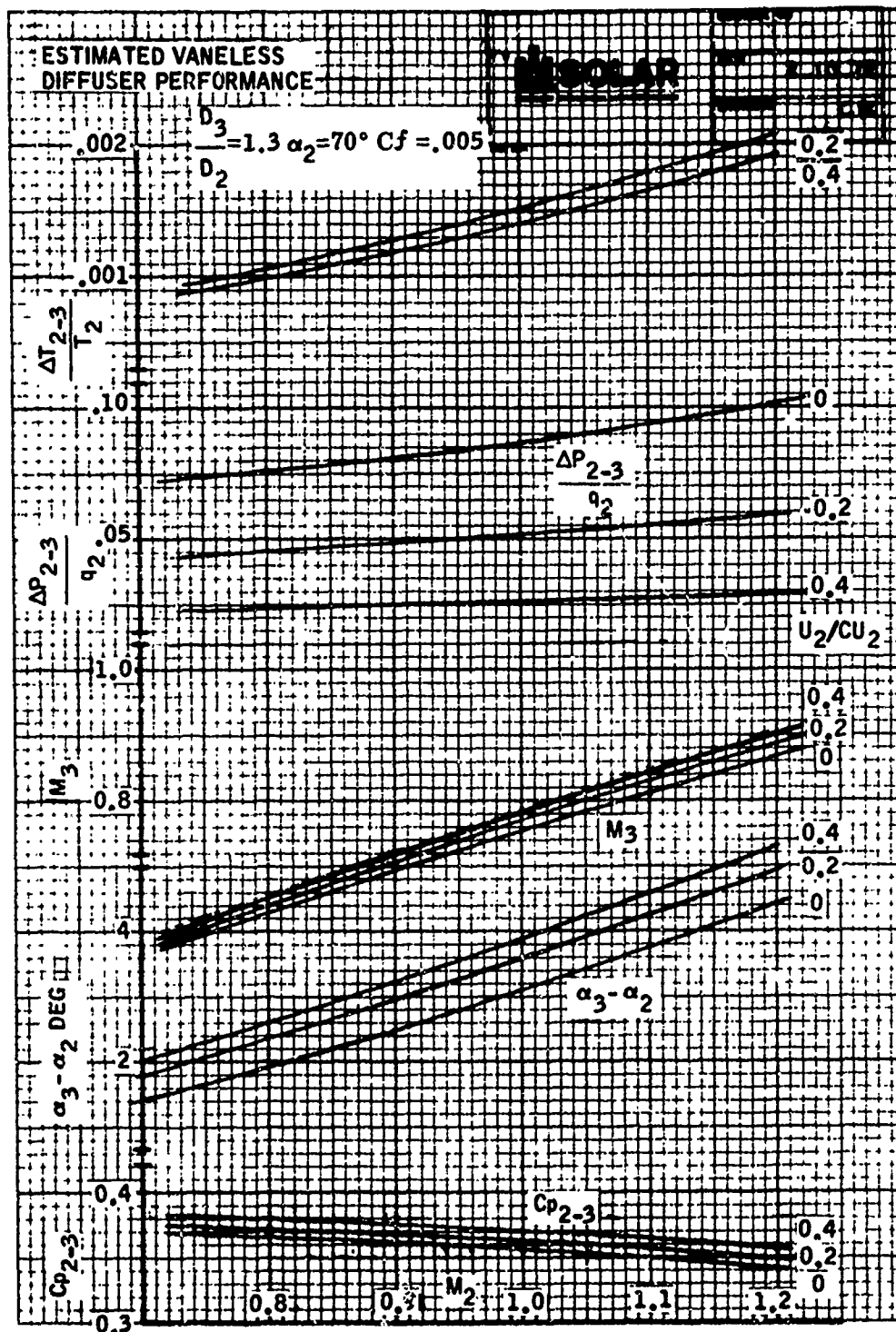
Figure 1.   Estimated Vaneless Diffuser Performance ($\alpha_2 = 70$ Degrees)

41
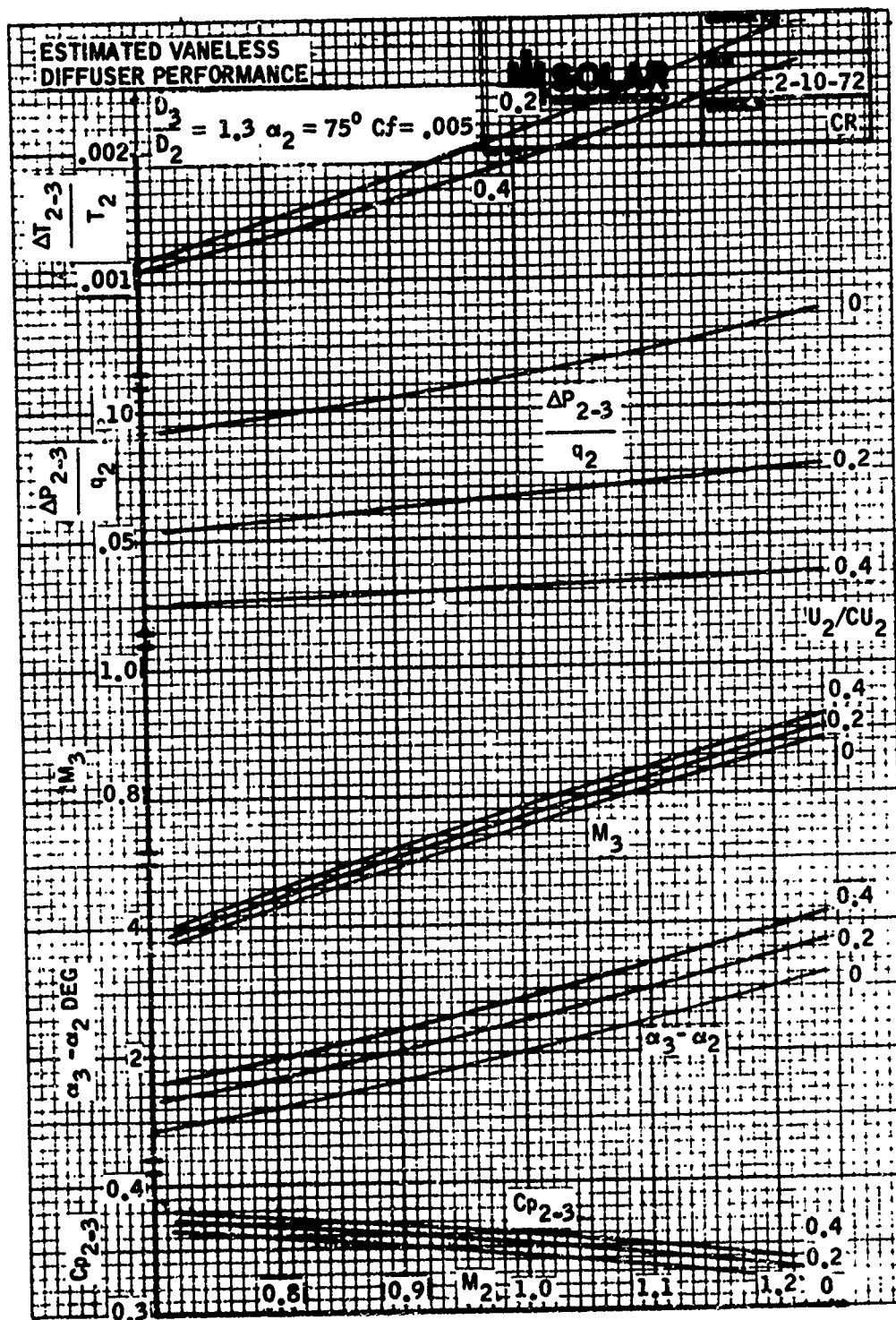
Figure 2. Estimated Vaneless Diffuser Performance (α_2 = 75 Degrees)
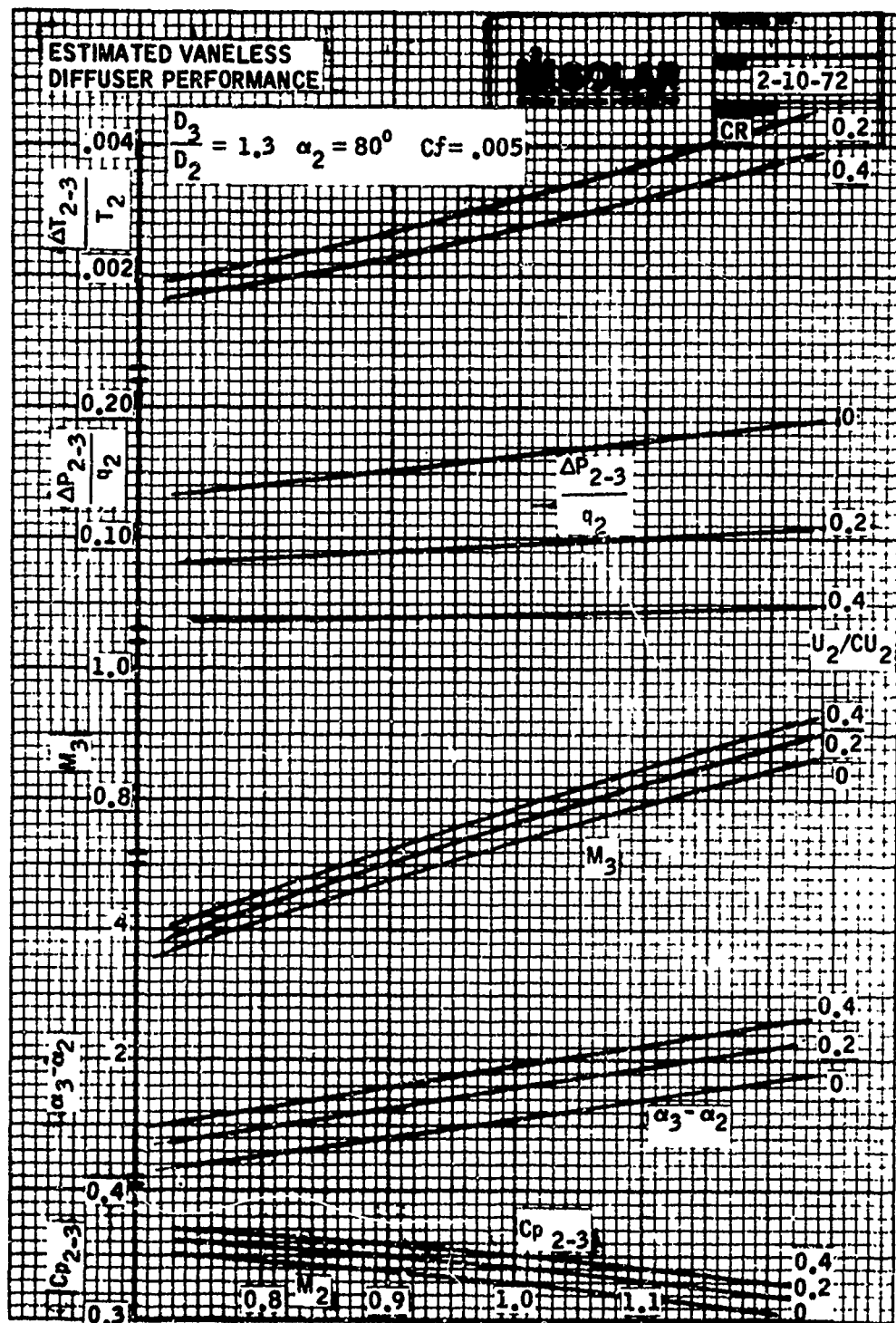
Figure 3. Estimated Vaneless Diffuser Performance ($\alpha_2 = 80$ Degrees)
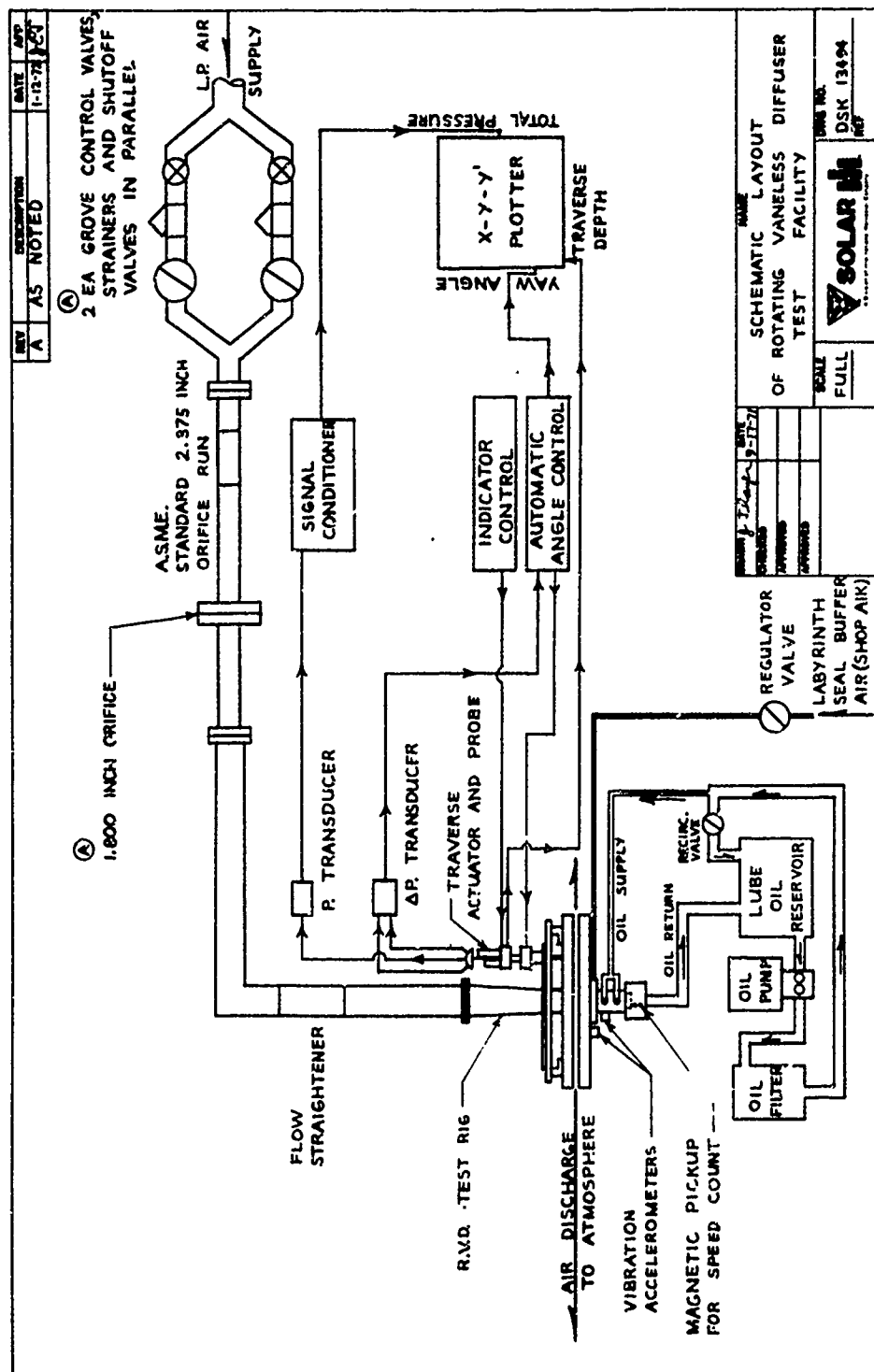
Figure 4. Rotating Vaneless Diffuser Test Facility, Schematic Layout
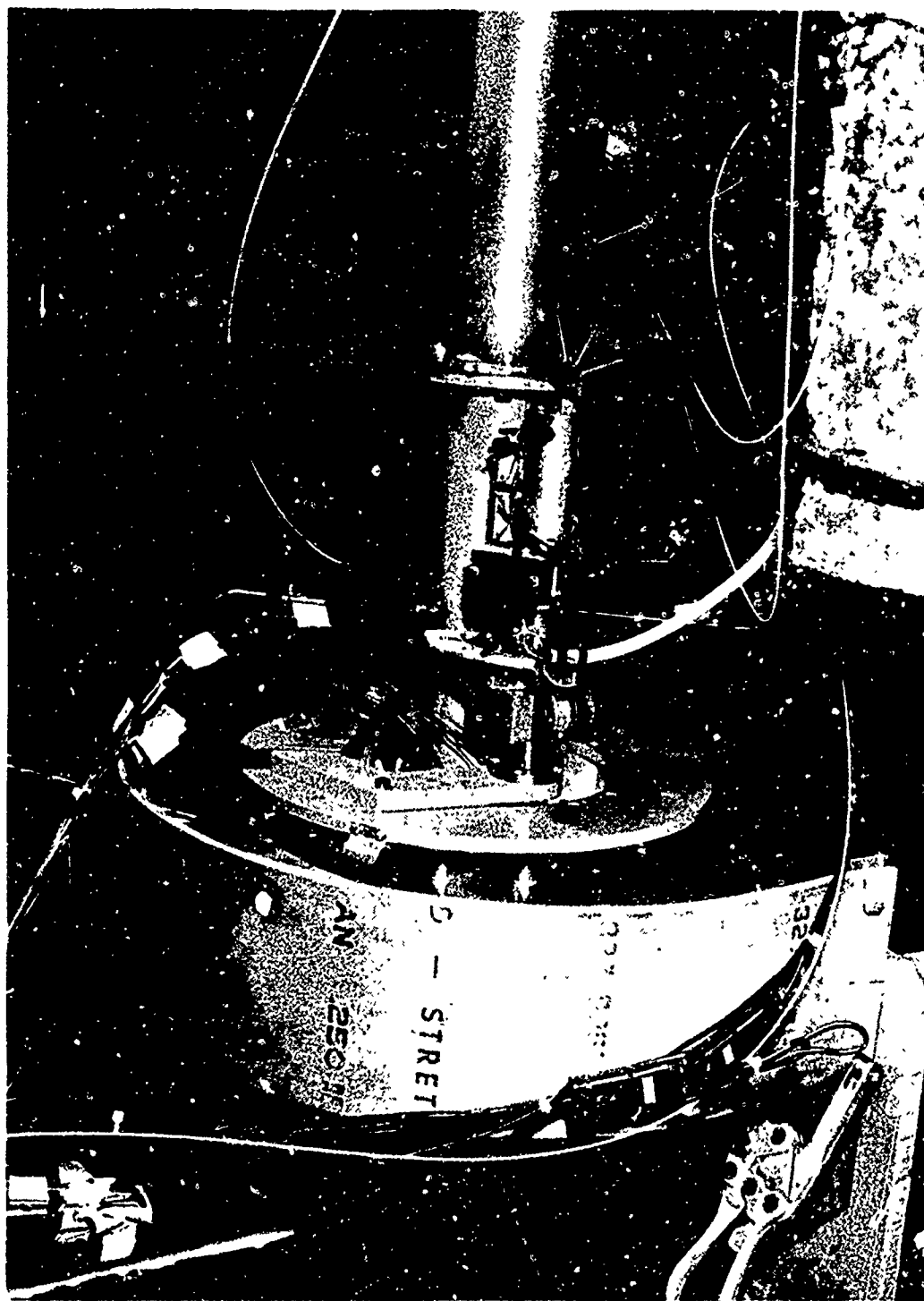
Figure 5. Rotating Diffuser Test Rig Total Pressure and Yaw Traversing Components
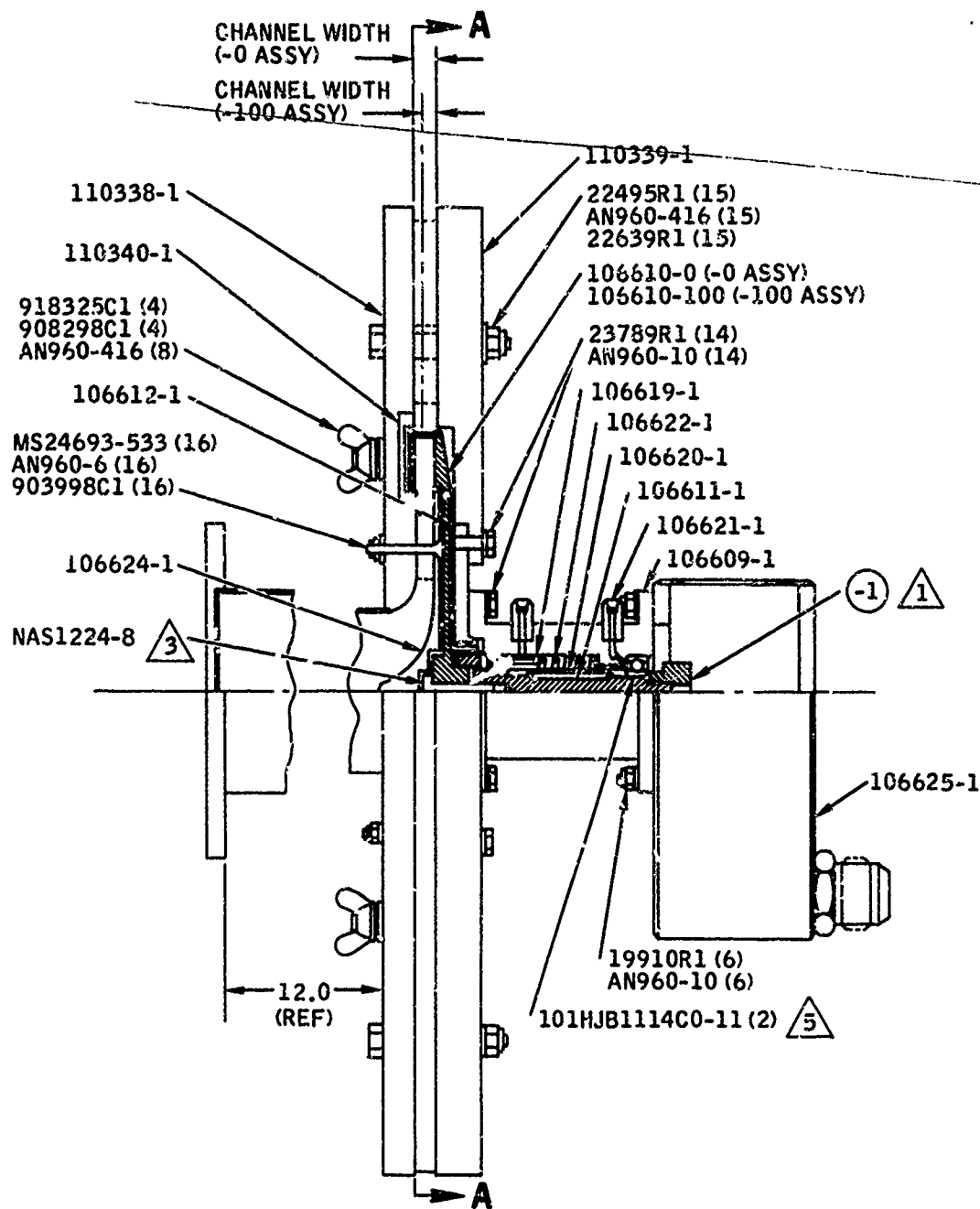
Figure 6.   Rotating Vaneless Diffuser Test Rig Cross-Section View

46

Figure 7. Cobra Head Traverse Probe

47
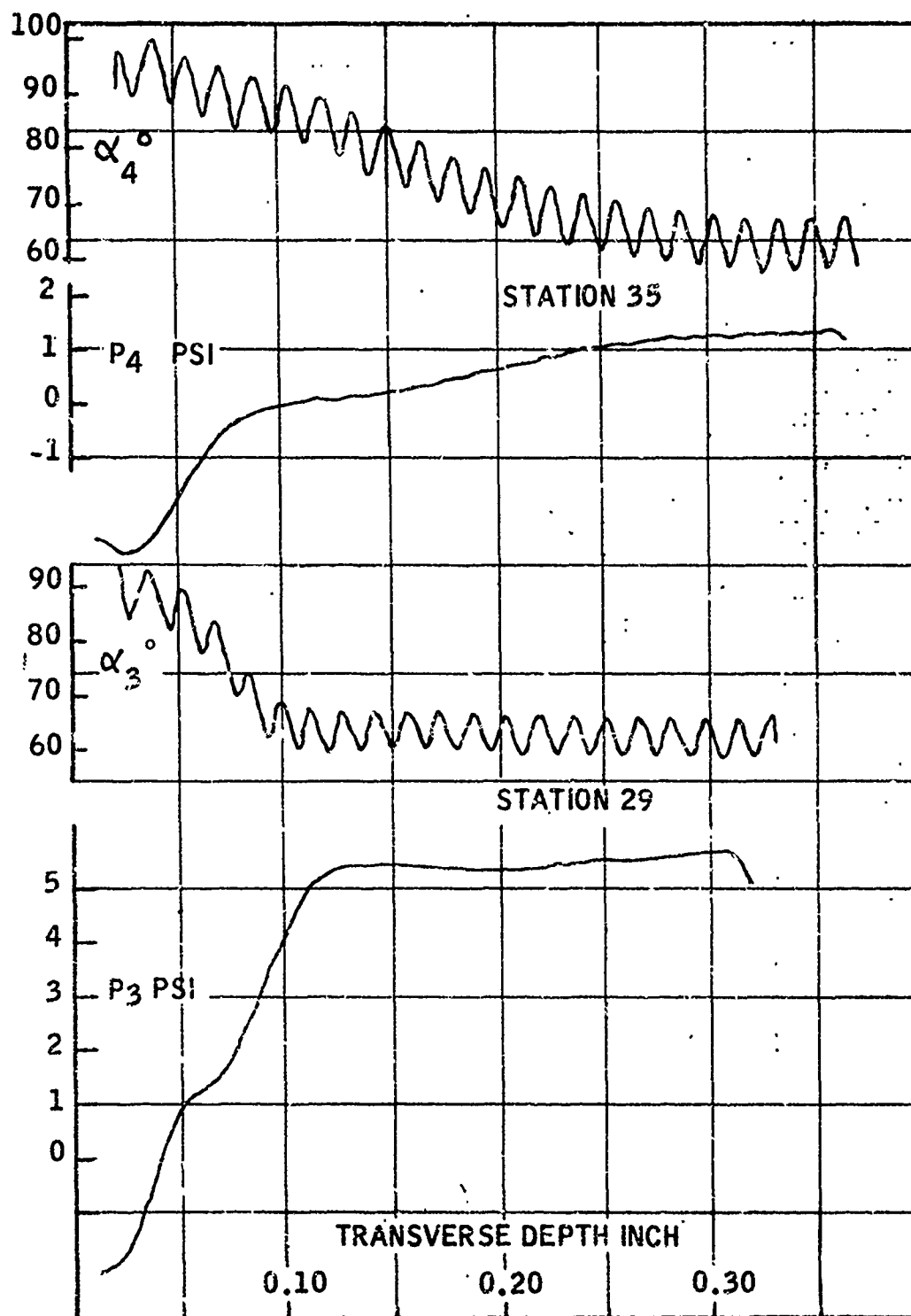
Figure 8. Typical Traverse, Data Point 36

FLOW PATH & INSTRUMENTATION STATIONS
R.V.D CONTINUATION STUDY.

15 VANES EQUALLY SPACED
REF: CS 18853

110° (C TO B)
(NOT TO SCALE)

14.0 DIA

10.4 P.C.DIA.

4.8° 4.8° 4.8° 4.8° 4.8°

.125
.125
.125

25.0°
(TAP A TO HOLE E)

36.0°
(HOLE C TO TAP D)

1.50   2.15

12°

12°

250 .350

10 P.C. DIA.

8.0 P.C. DIA.
(MAXIMUM)

5.6 P.C. DIA.
(MINIMUM)

15°

76°

DIRECTION OF ROTATION
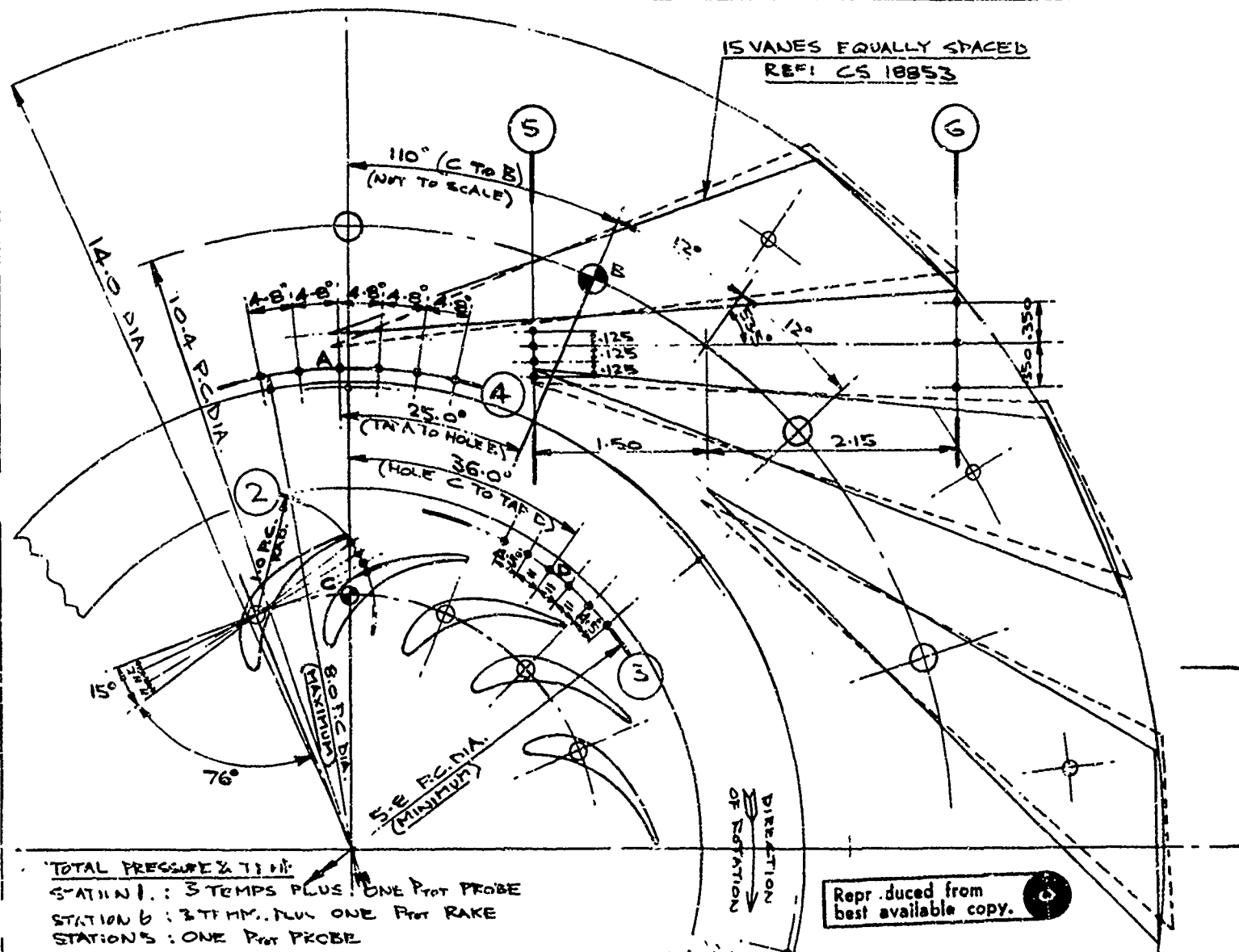
TOTAL PRESSURE & TEMP.
STATION 1 : 3 TEMPS PLUS ONE P_{TOT} PROBE
STATION 6 : 3 TEMP PLUS ONE P_{TOT} RAKE
STATION 5 : ONE P_{TOT} PROBE

WALL STATIC TAPS
STATION 2 : 4 AS SHOWN, READ 3
STATION 3 : 6 AS SHOWN, READ 5
STATION 4 : 6 AS SHOWN, READ 5
STATION 5 : 4 AS SHOWN, READ 3&4
STATION 6 : 3 AS SHOWN, READ 3

TRAVERSES STATIONS 3 & 4
CONTINUOUS TRAVERSING CAPABILITY REQUIRED (24° MIN) WITH
25 DATA POINTS 1 PR. STATION, TOTAL PRESSURE & FLOW ANGLE
5 POINTS RADIAL (SPACED FOR EQUAL AREAS)
5 POINTS CIRCUMFERENTIAL (SPACED LIKE
WALL TAPS)

ALL DIMENSIONS
DIMENSIONS TO
EXCEPT AS NO
STATIC TAPS

& INSTRUMENTATION STATIONS CONTINUATION STUDY.

VANES EQUALLY SPACED
REF: CS 18853

NO STEPS UP IN DIRECTION OF FLOW ON EITHER SURFACE

7 — AMBIENT

6 — VANED DIFFUSER EXIT

.360/.361

.240/.241

5 — VANED DIFFUSER THROAT

4 — R.V.D. EXIT

RADIAL CLEARANCE BOTH SIDES

.349/.351

.229/.231

3 — R.V.D. INLET

2 — SWIRL NOZZLE THROAT

.320/.321

.200/.201

1

FLOW DIRECTION

6.50
(NOT TO SCALE)

2.15

G

DIRECTION

ALL DIMENSIONS IN INCHES.
DIMENSIONS TO DRAWING No. 106607
EXCEPT AS NOTED.
STATIC TAPS .030 DIA MAX.
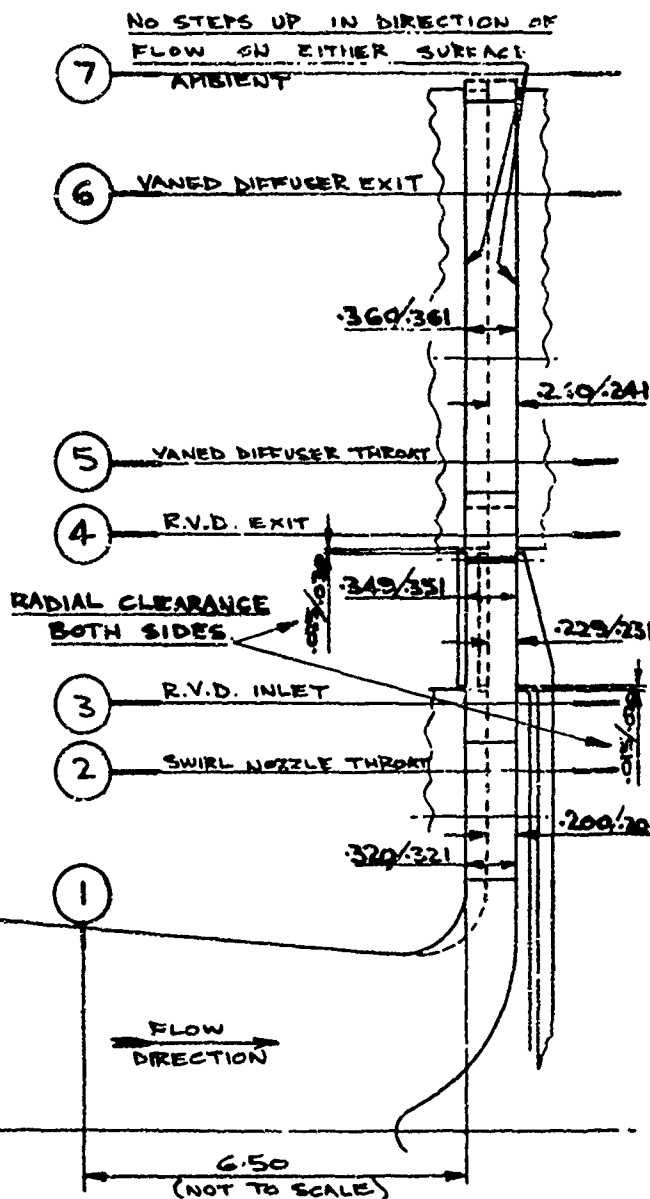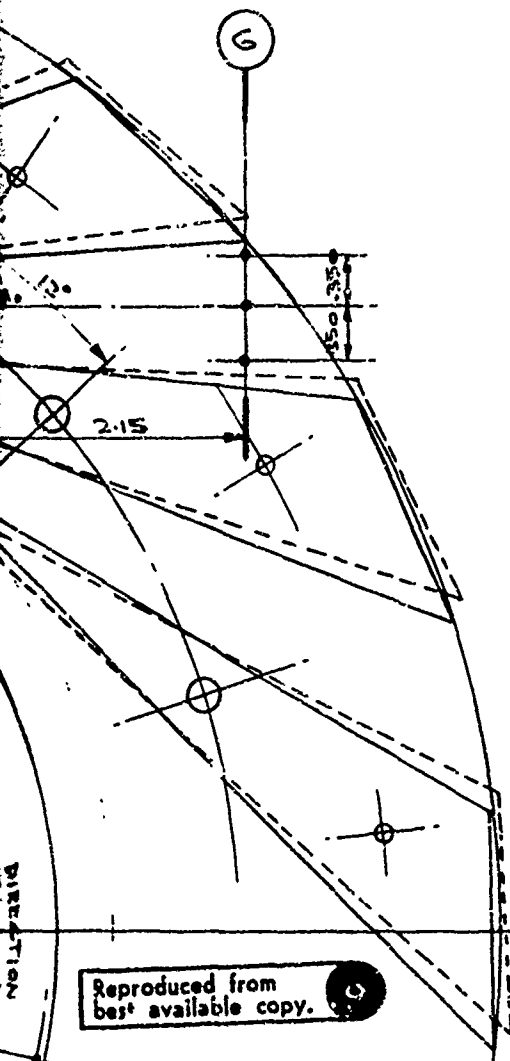
Figure 9. Flow Path and Instrumentation Stations
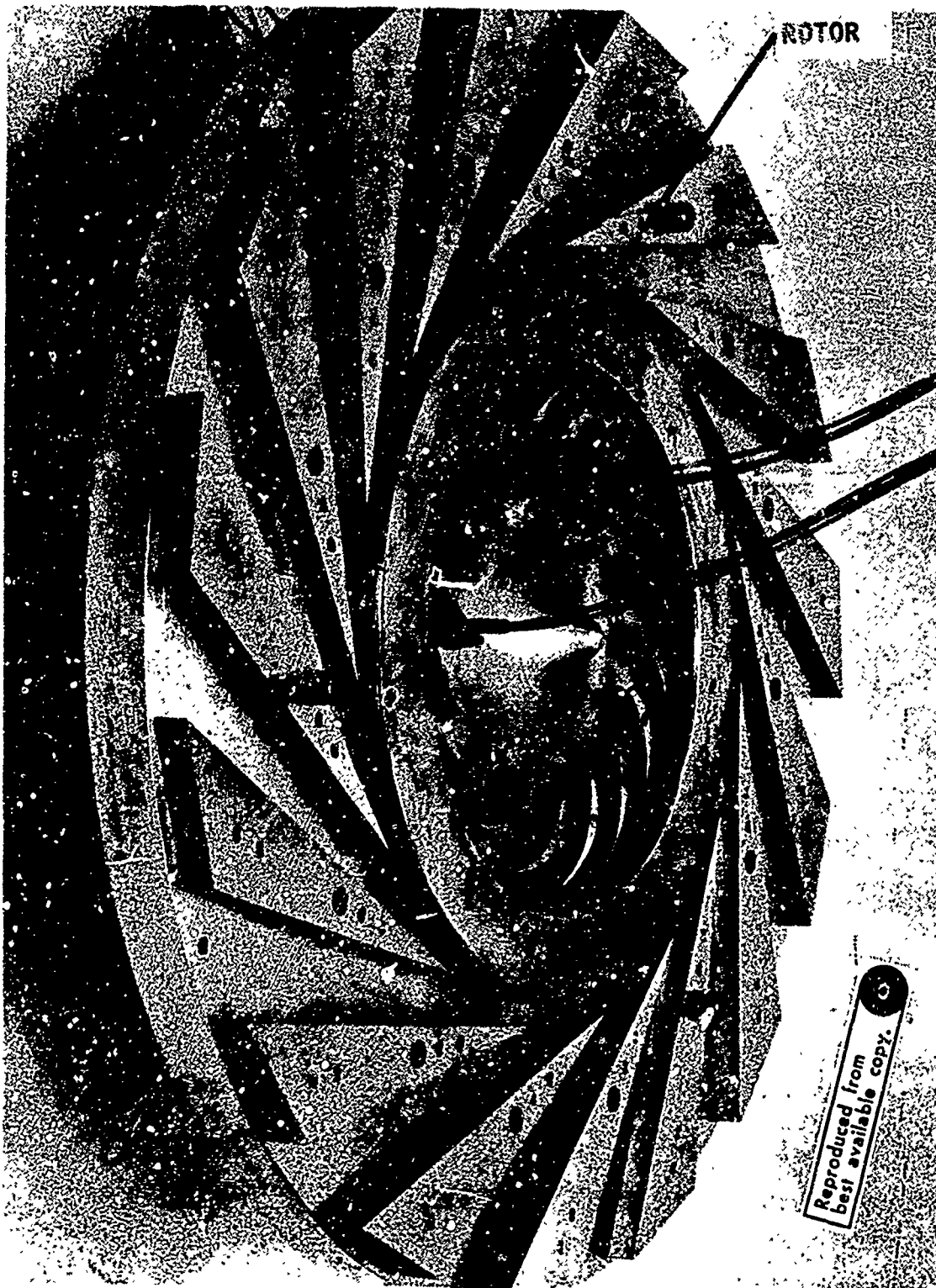
ROTOR

Figure 10. Diffuser Test Rig

.230.

.350.

Figure 11. Rotating Diffuser Rotors
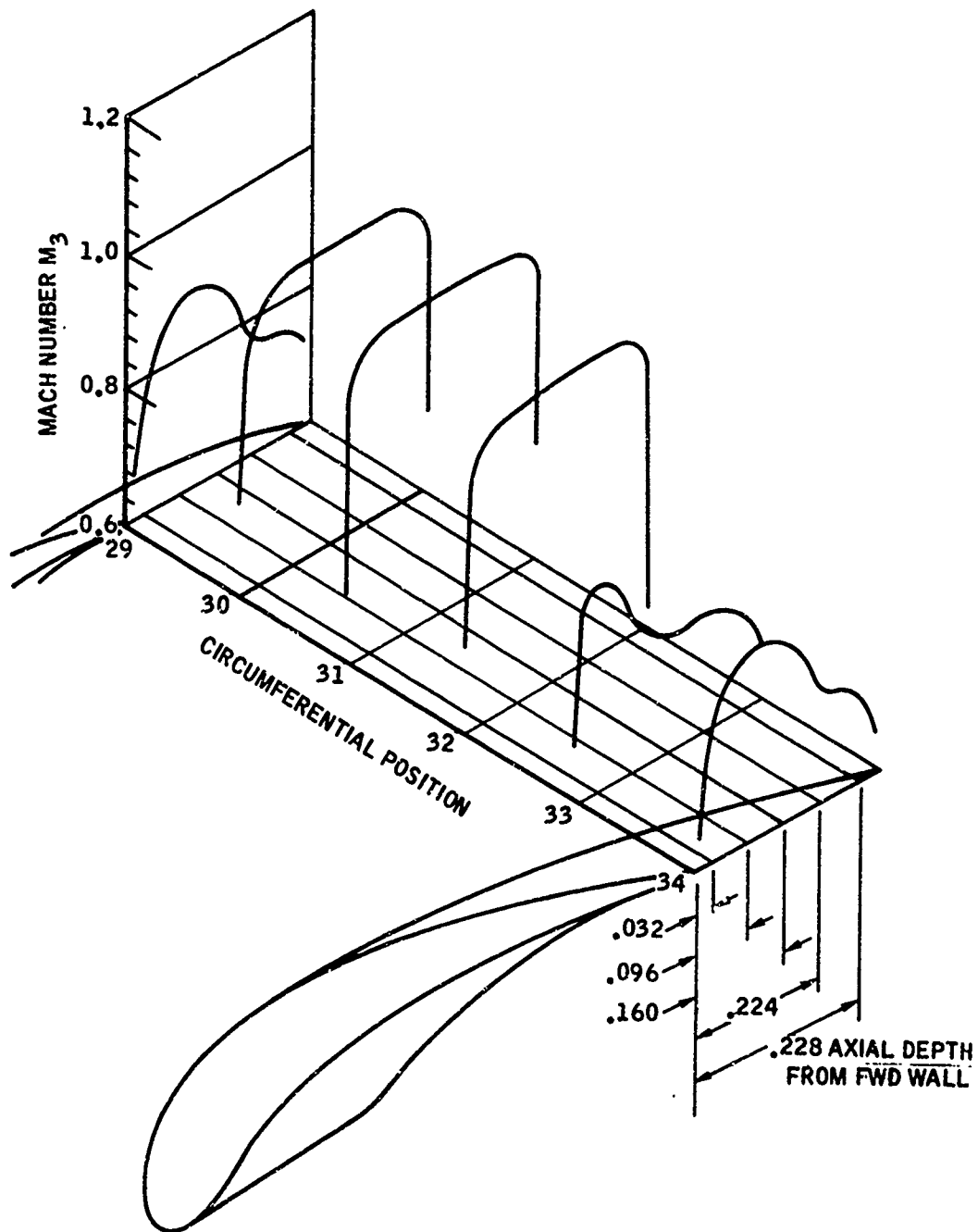
Figure 12.   Rotating Diffuser Swirl Nozzle Traverse Area
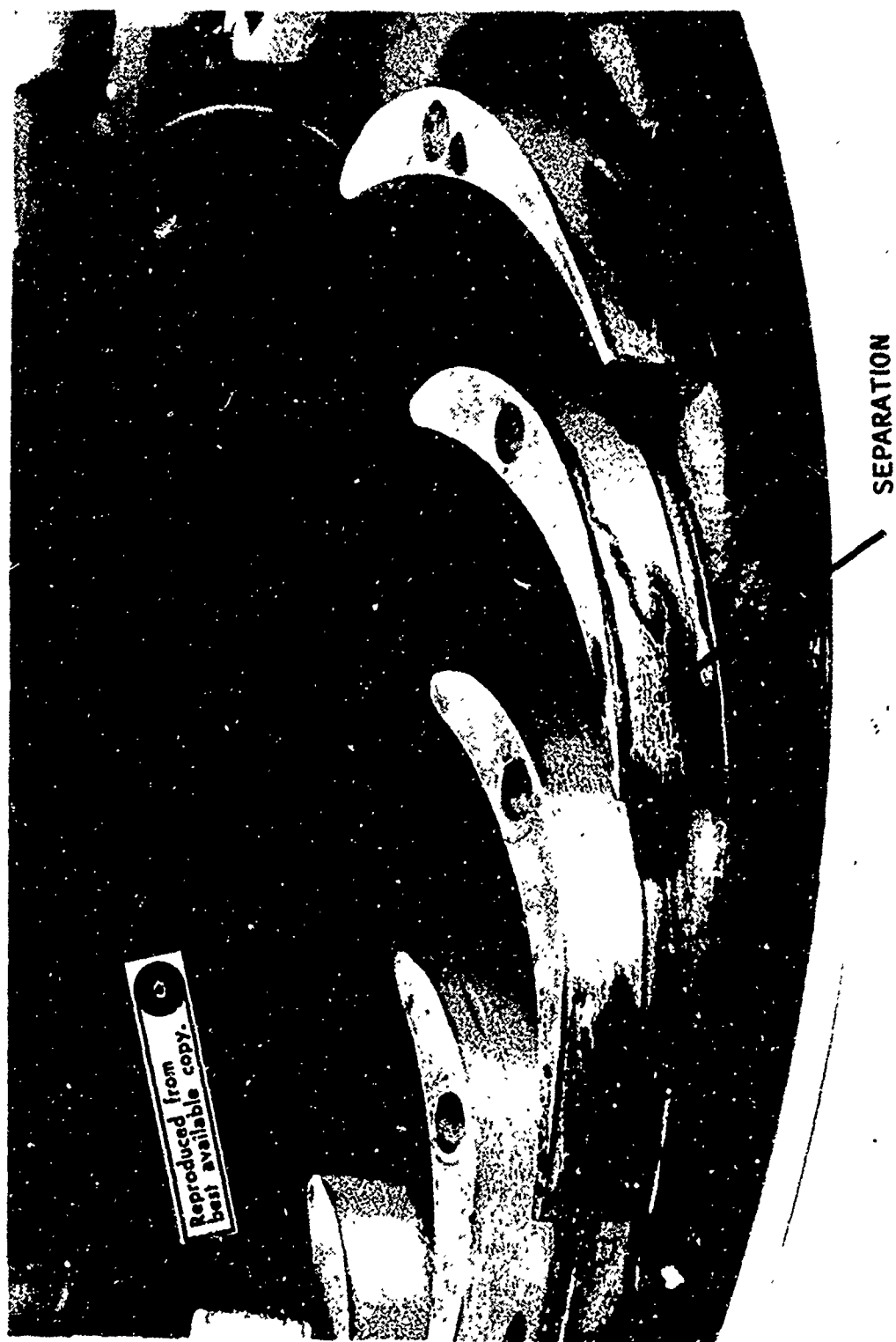
Figure 13. Nozzle Suction Surface Separation

SEPARATION

54
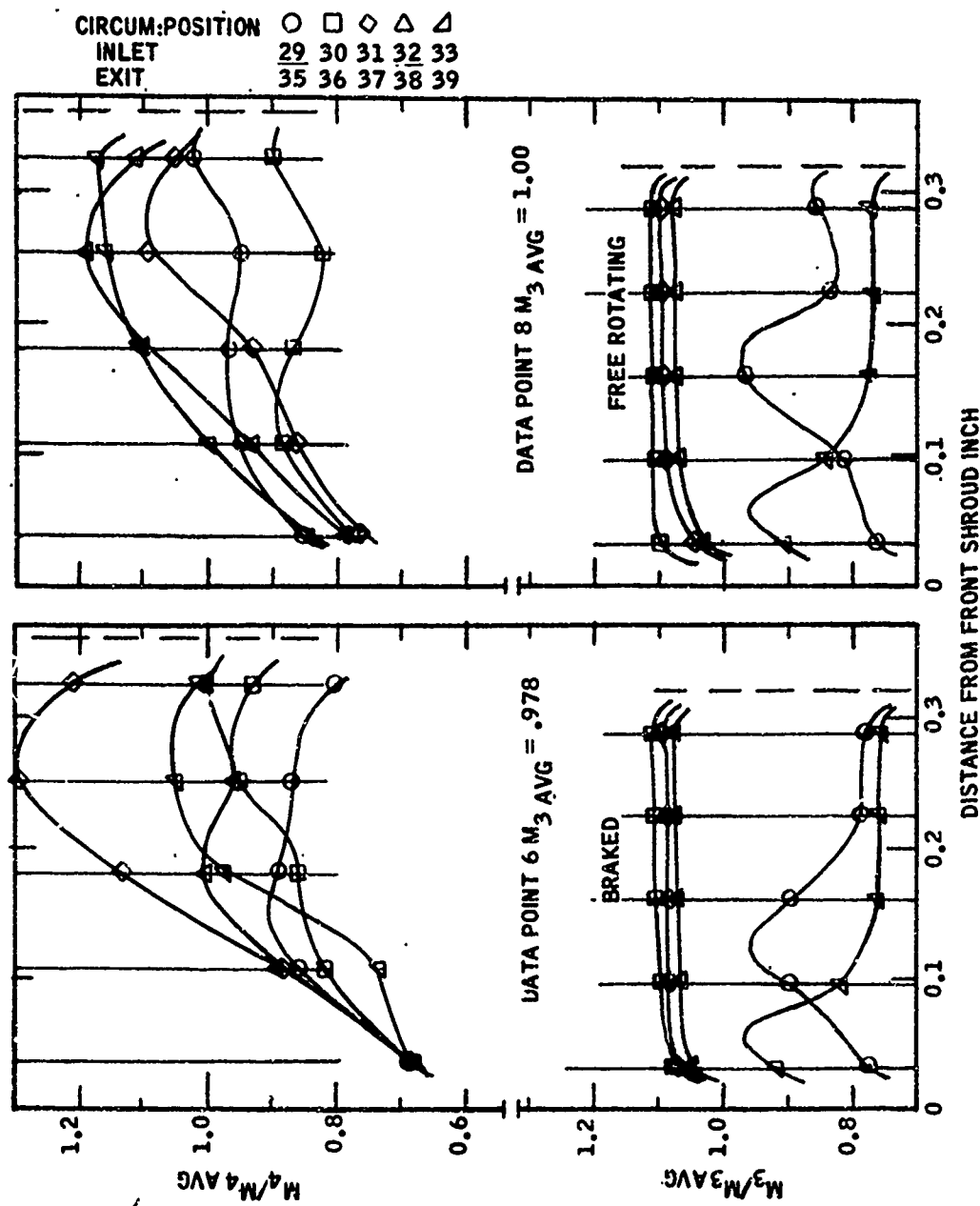
Figure 14. Rotating Vaneless Diffuser Traverse Data (Sheet 1 of 5)

55
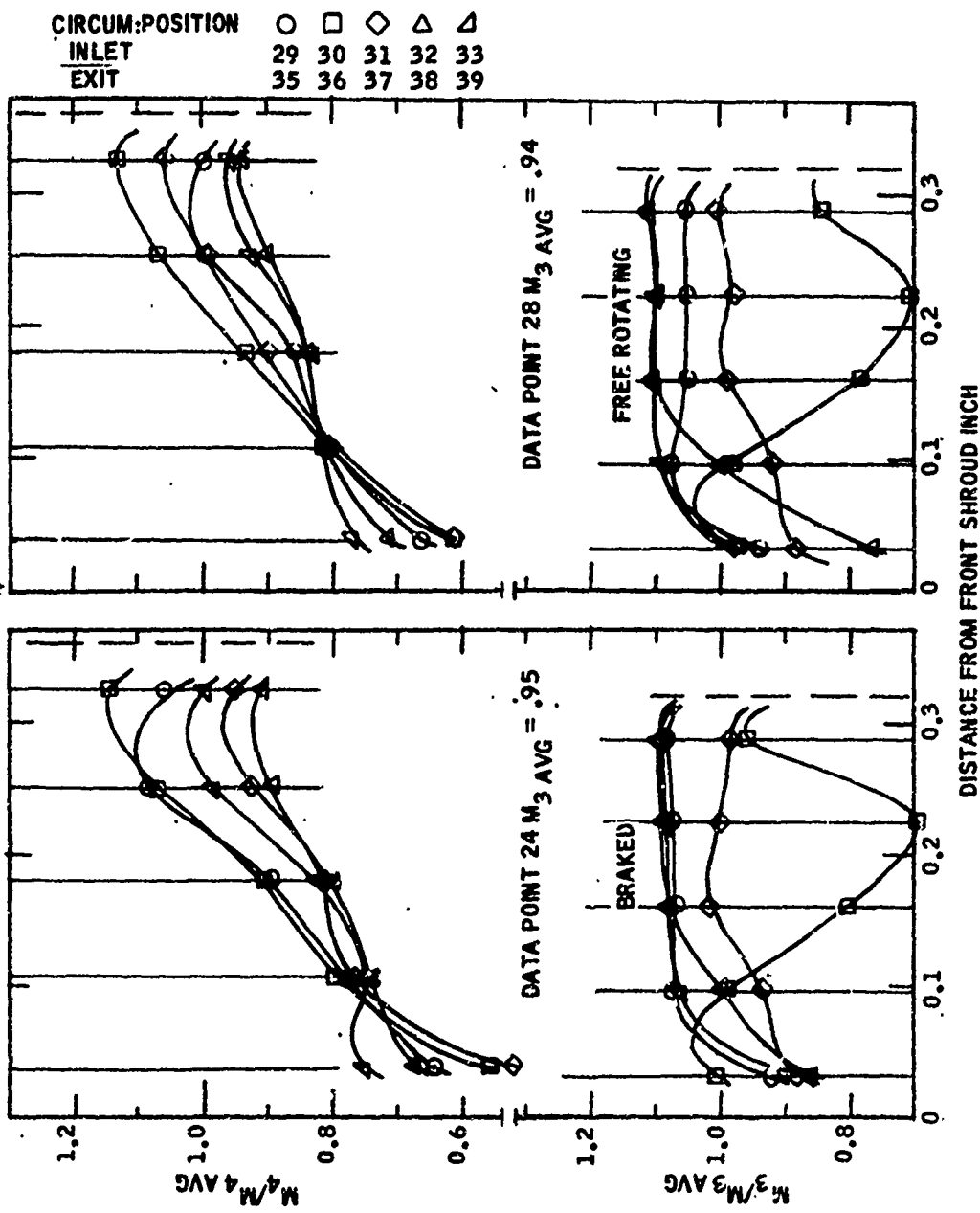
Figure 15. Rotating Vaneless Diffuser Traverse Data (Sheet 2 of 5)
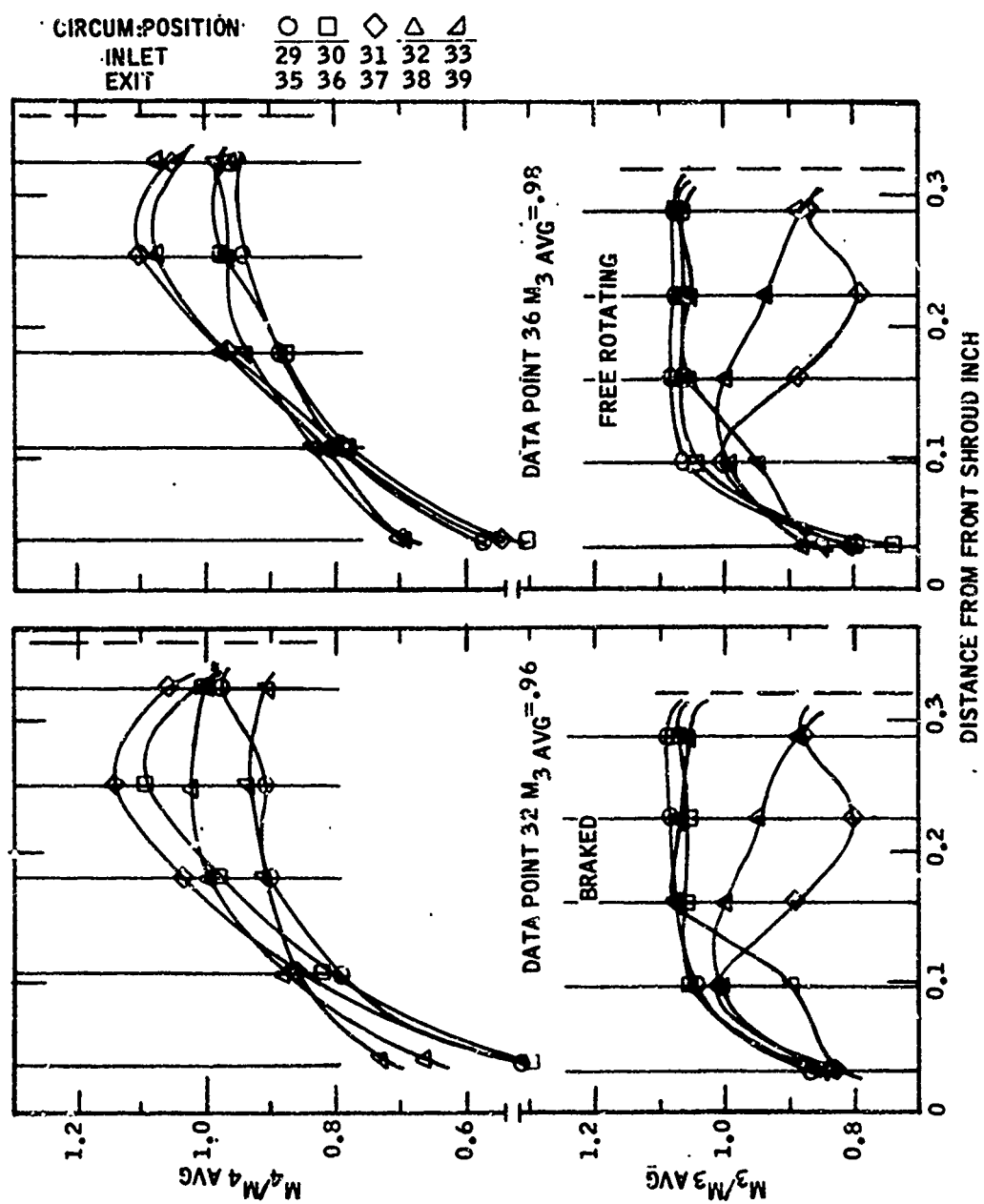
Figure 16. Rotating Vaneless Diffuser Traverse Data (Sheet 3 of 5)

57
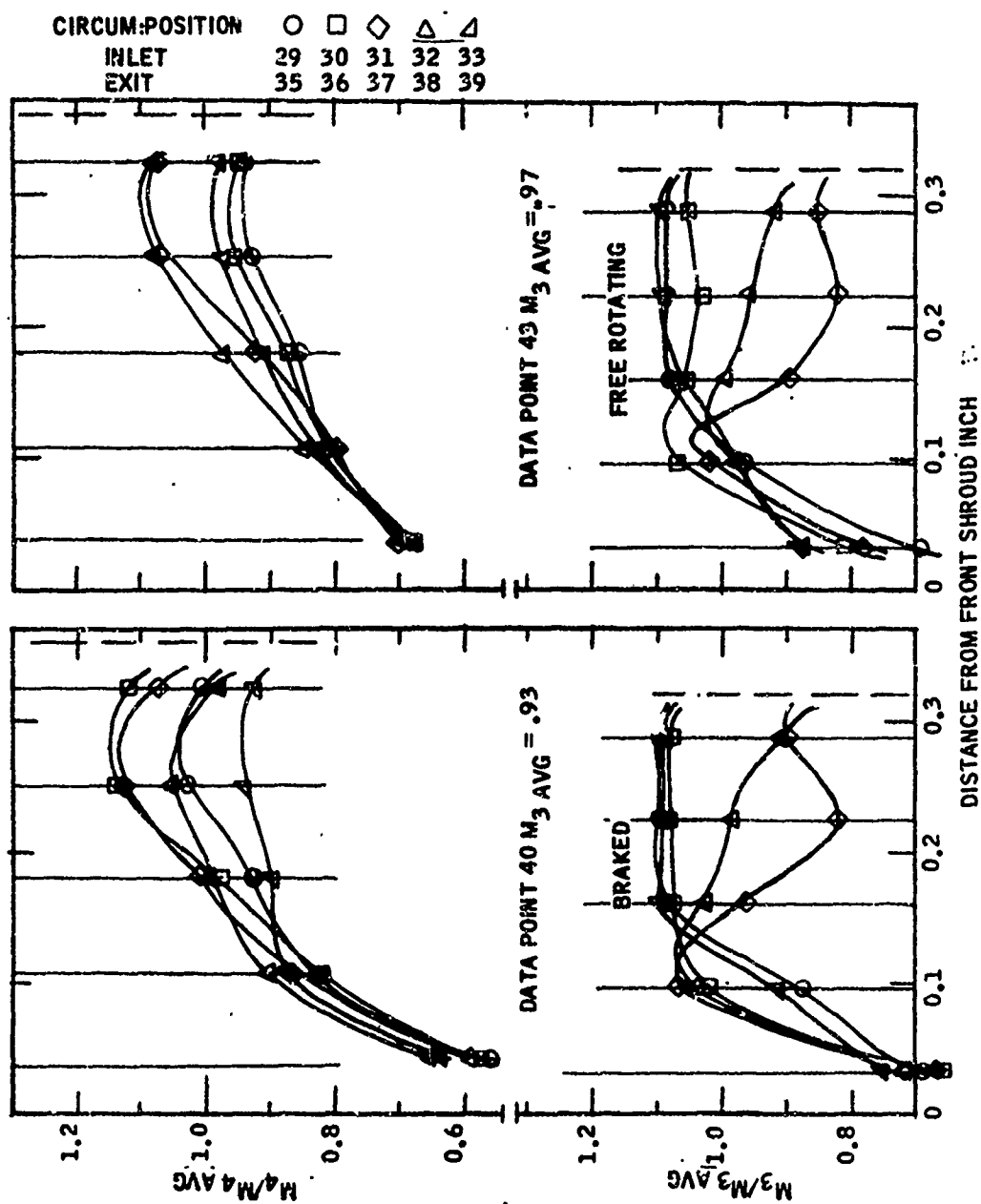
Figure 17. Rotating Vaneless Diffuser Traverse Data (Sheet 4 of 5)
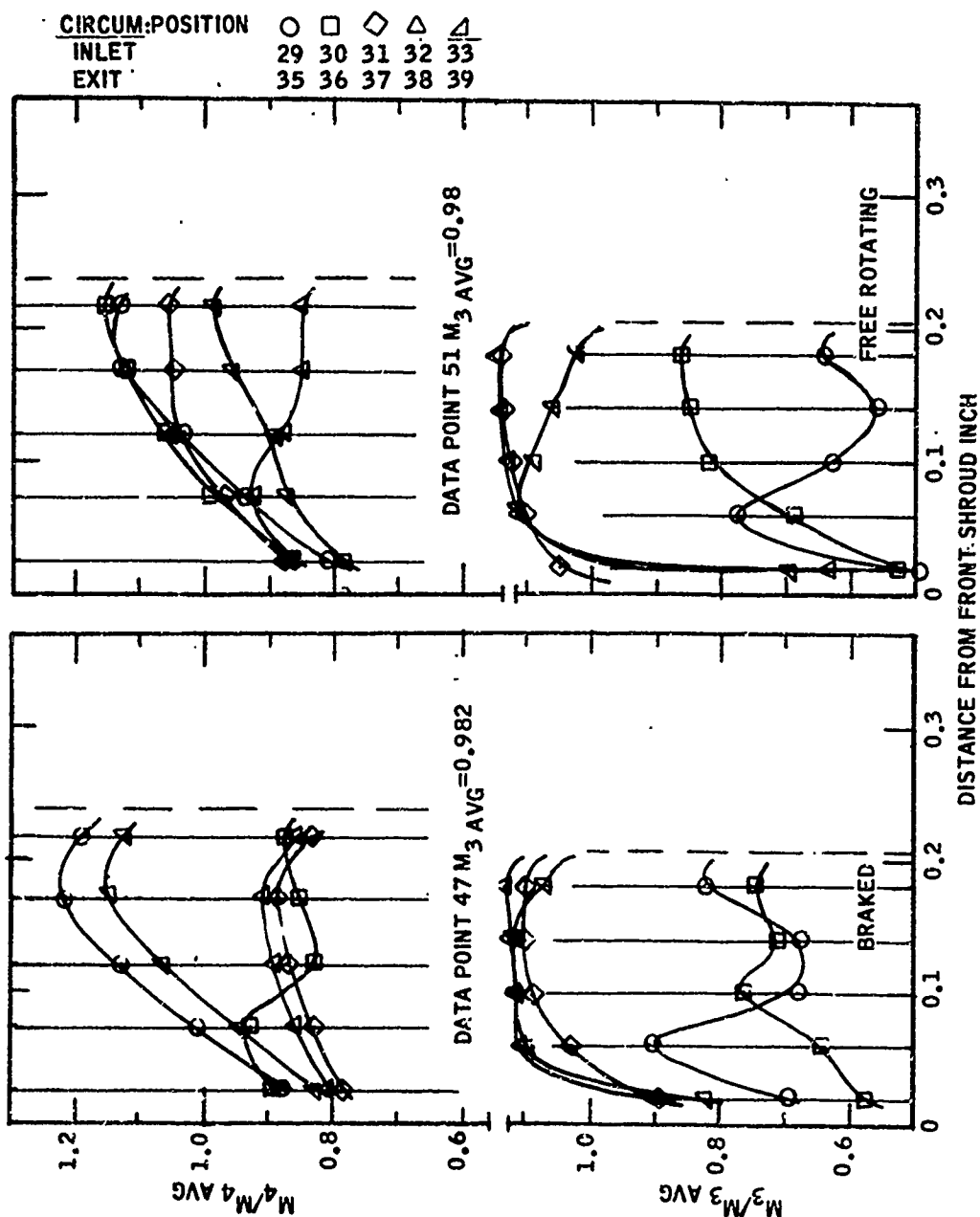
Figure 18. Rotating Vaneless Diffuser Traverse Data (Sheet 5 of 5)
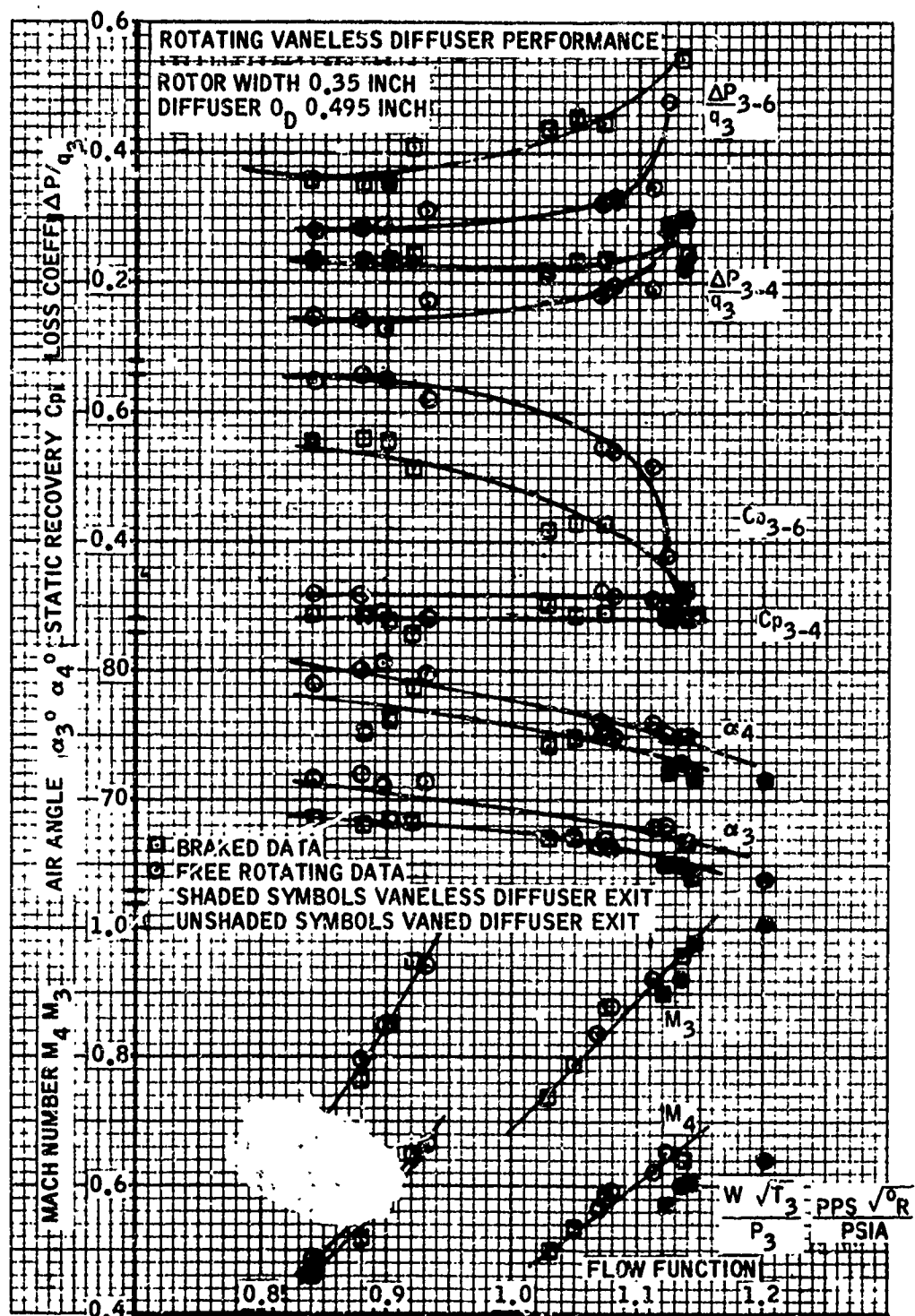
Figure 19. Rotating Vaneless Diffuser Performance, Rotor Width 0.35 in.,
Diffuser OD 0.495 in.

PRESSURE RATIO 6-10
VANELESS DIFFUSER DIA RATIO 1.2-1.3
Cp BASE 0.65
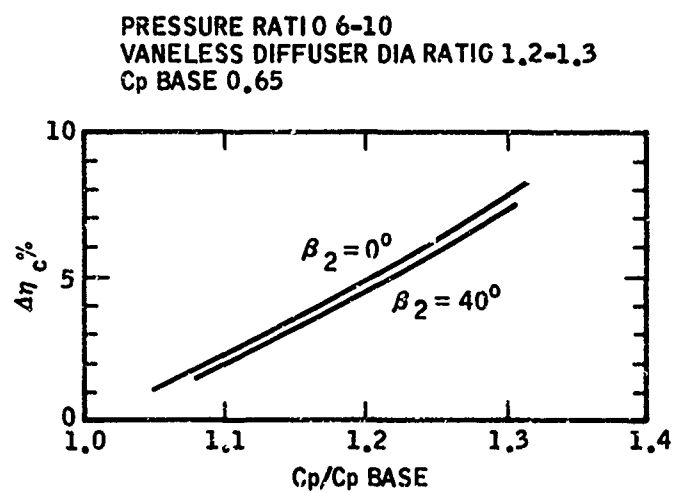
Figure 20. Typical Effect of Diffuser Static Pressure
Recovery Cp on Compressor Overall Efficiency
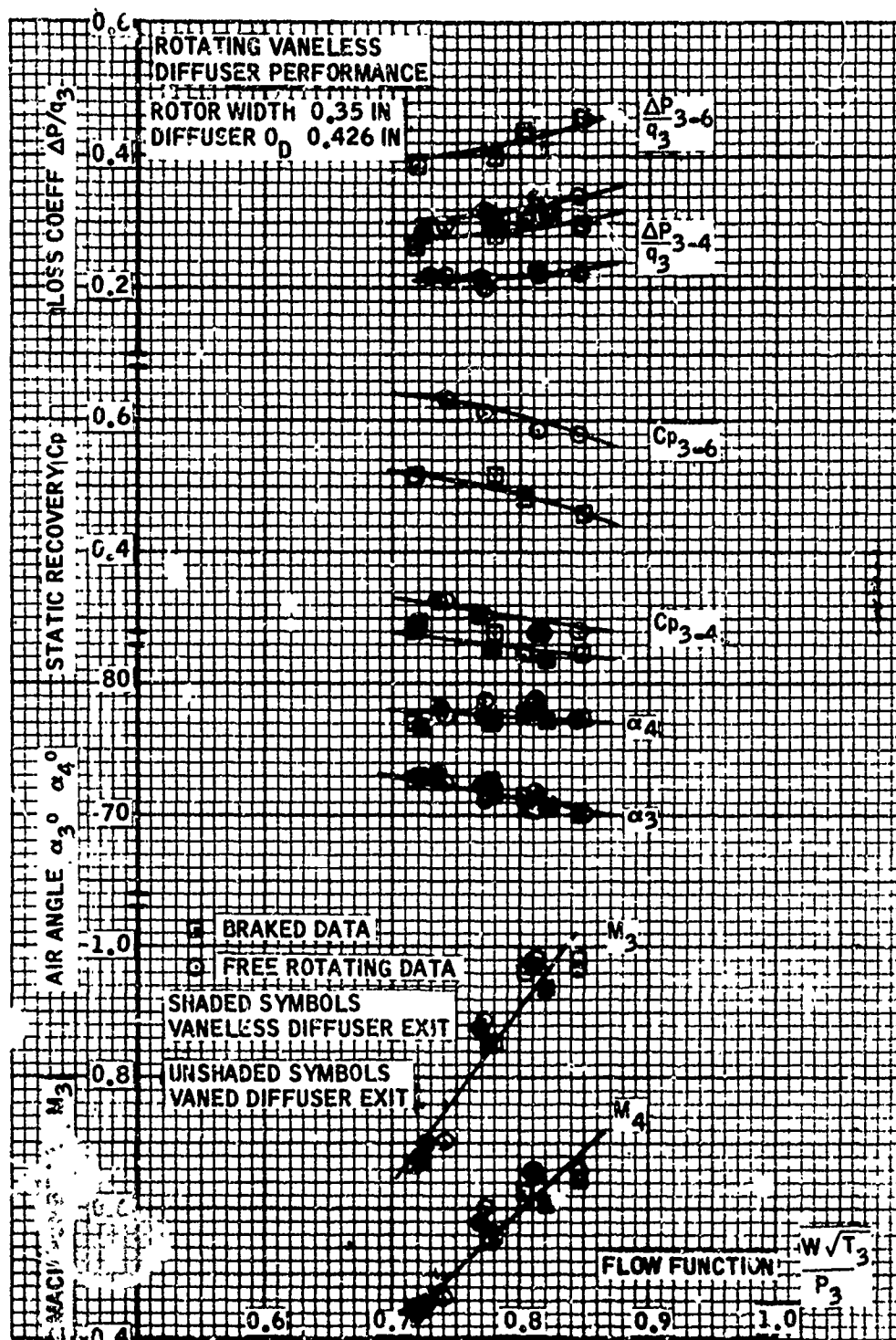
Figure 21. Rotating Vaneless Diffuser Performance, Rotor Width 0.35 in.
Diffuser OD 0.426 in.
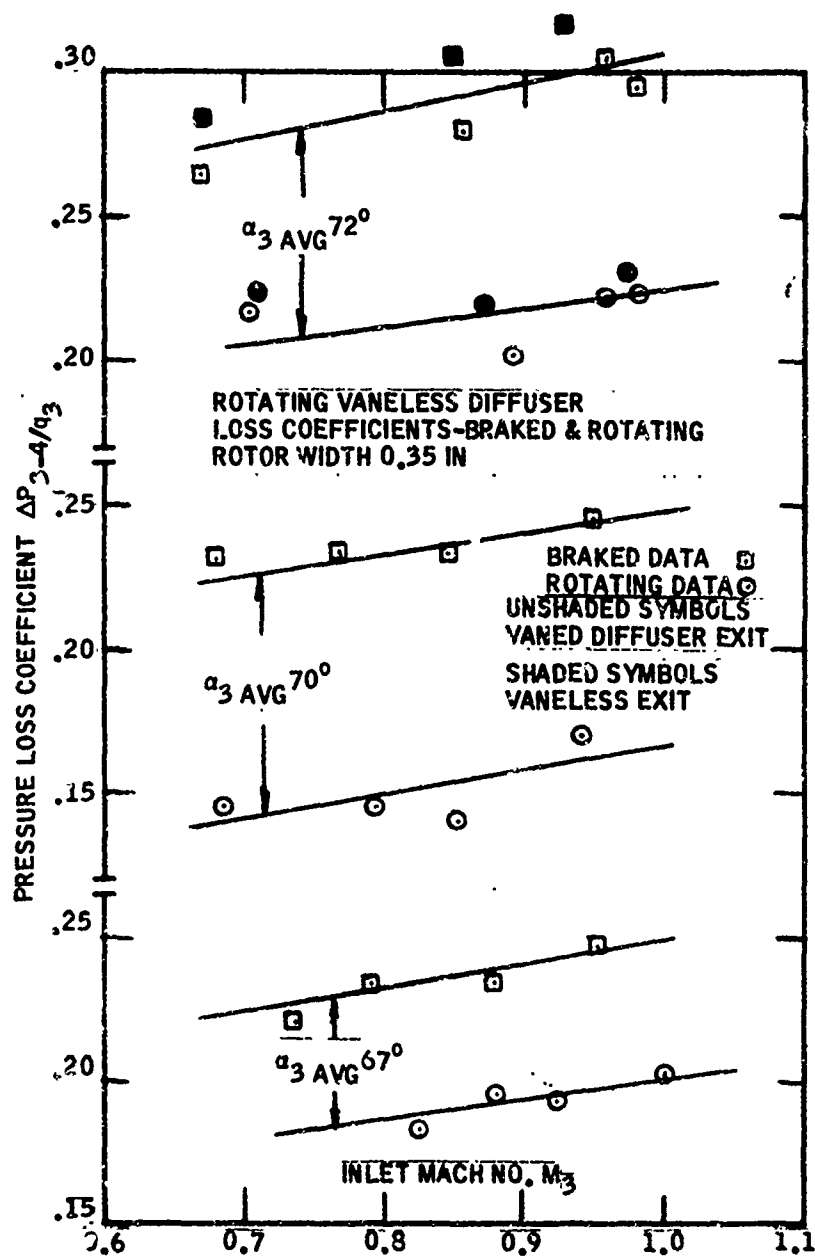
Figure 22. Rotating Vaneless Diffuser Loss Coefficients, Braked
and Rotating, Rotor Width 0.35 in.
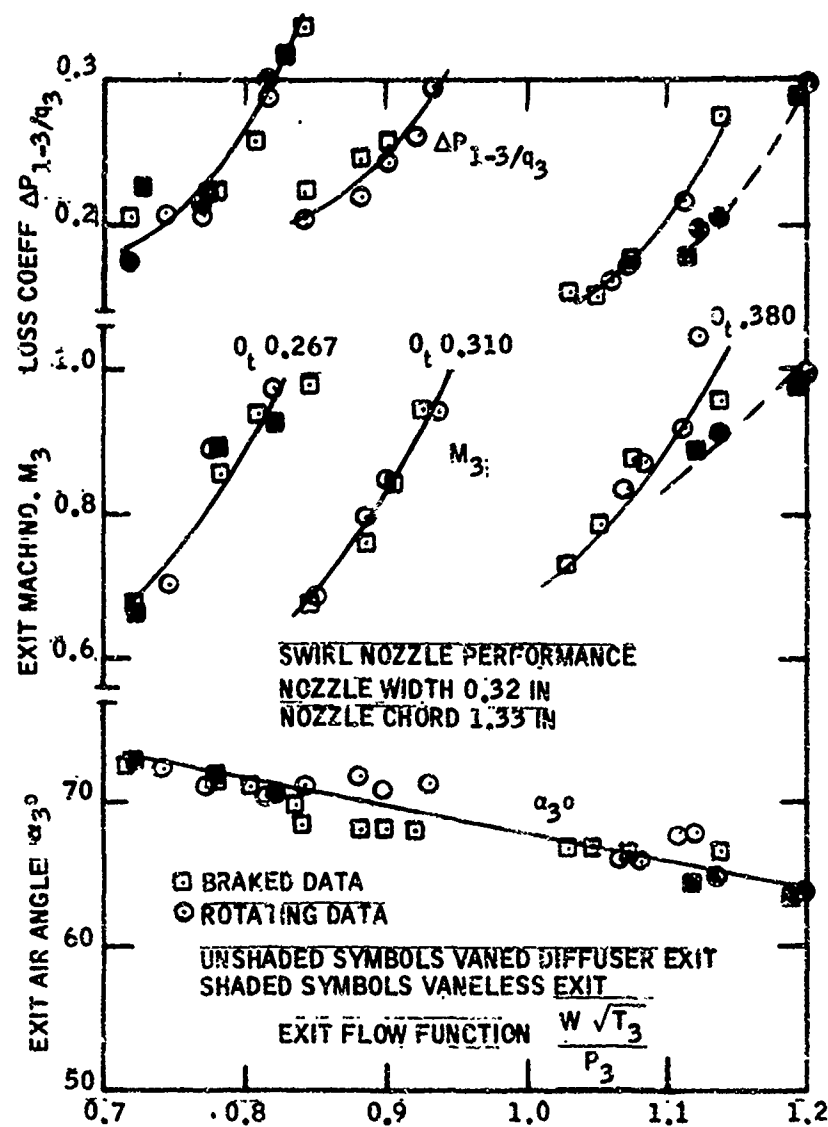
Figure 23. Swirl Nozzle Performance, Nozzle Width 0.32 in.,
Nozzle Chord 1.33 in.
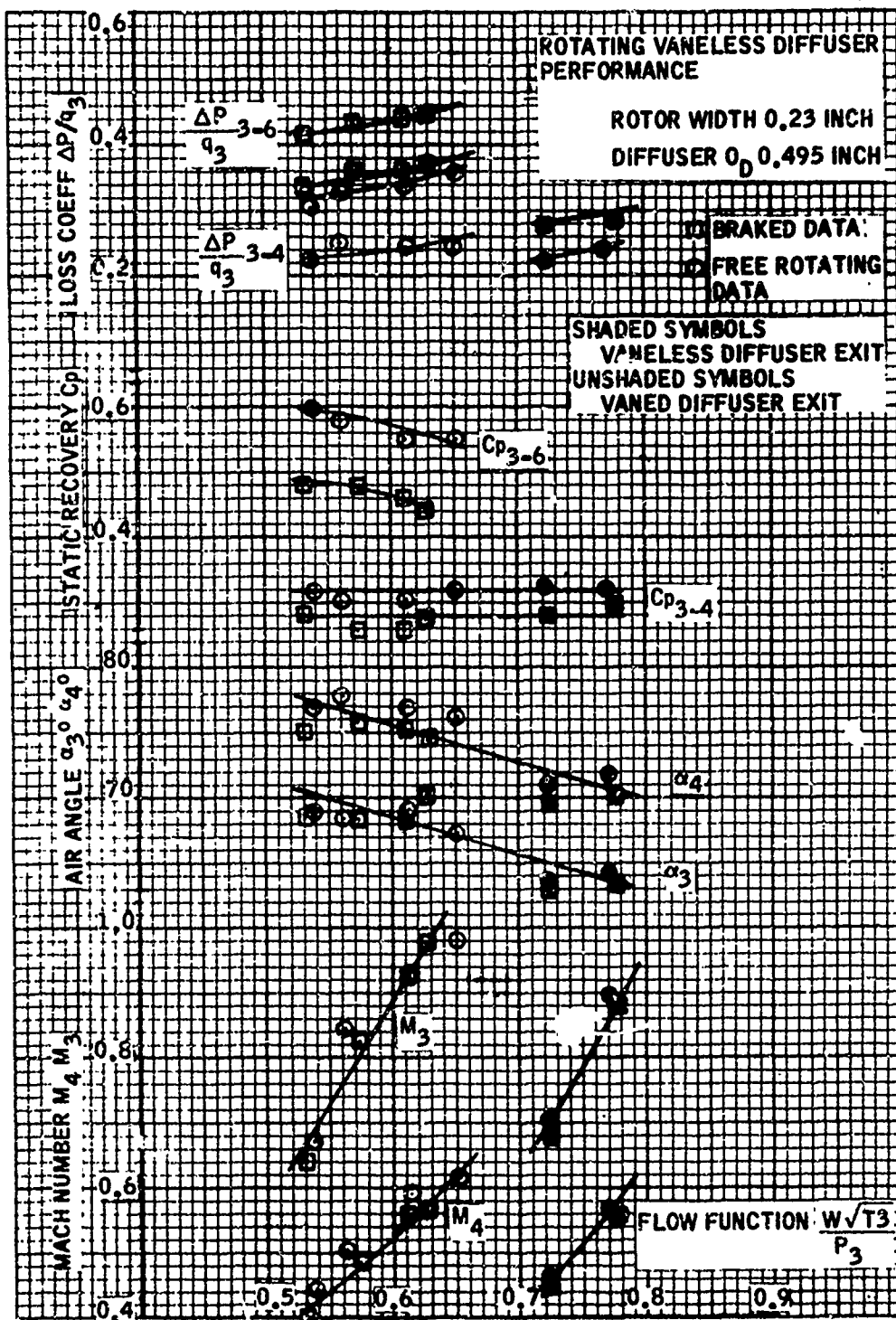
Figure 24.   Rotating Vaneless Diffuser Performance, Rotor Width 0.23 in.,
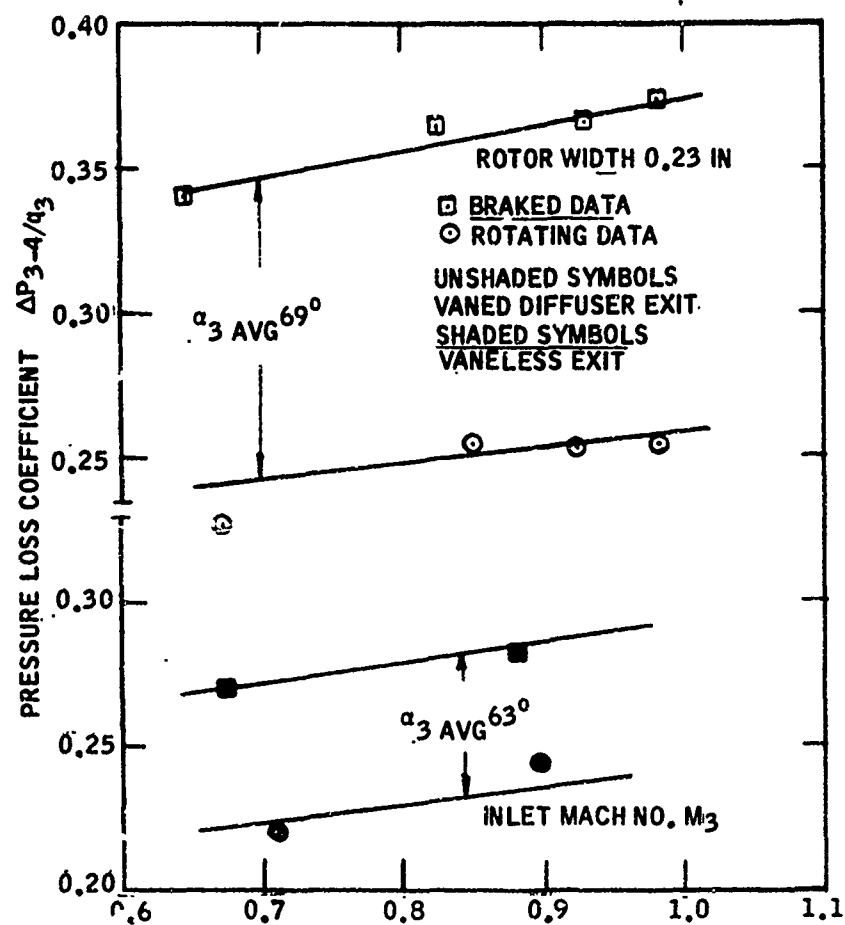Diffuser OD 0.495 in.

Figure 25. Rotating Vaneless Diffuser Loss Coefficients, Rotor Width 0.23 in.

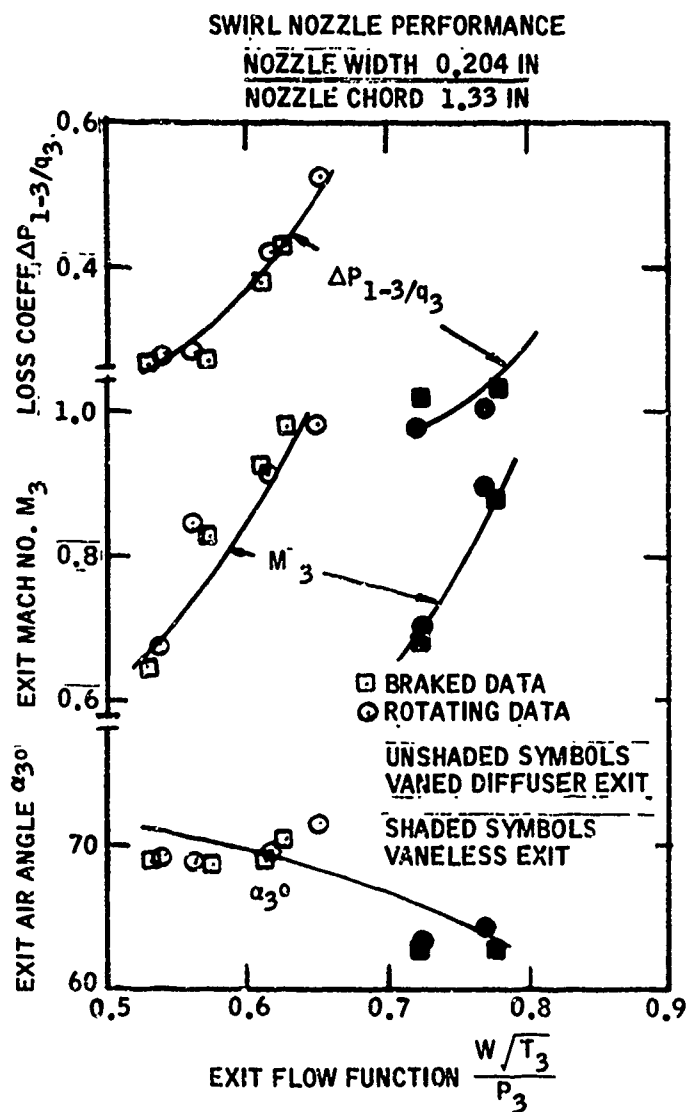SWIRL NOZZLE PERFORMANCE
NOZZLE WIDTH 0.204 IN
NOZZLE CHORD 1.33 IN

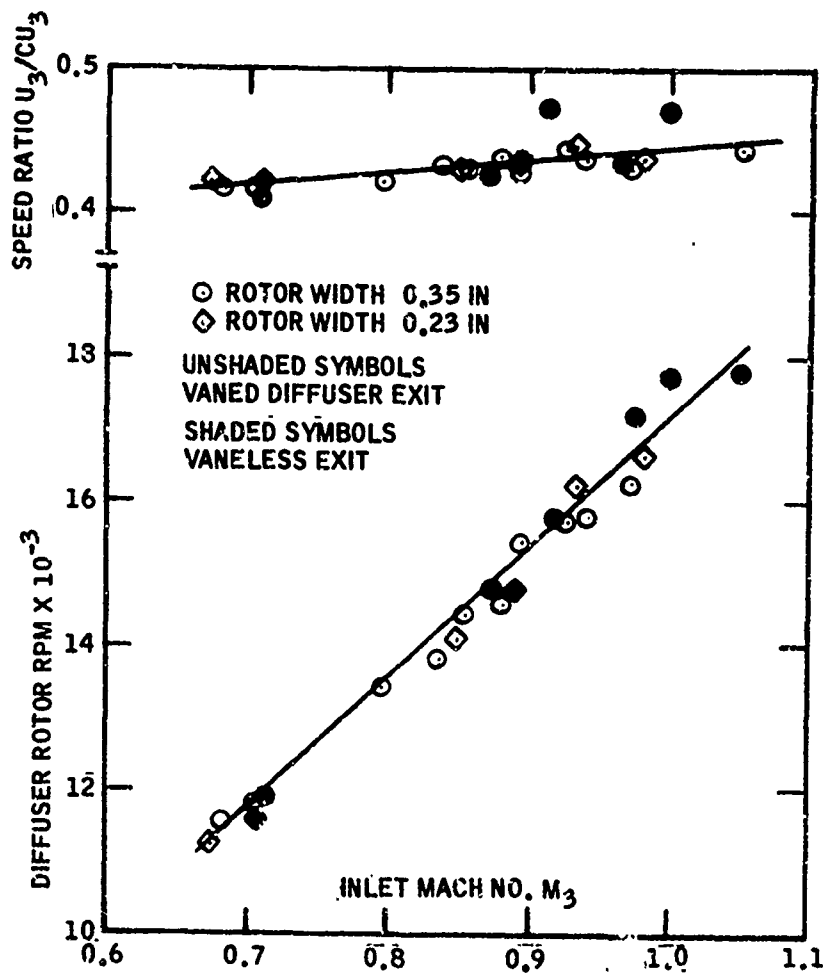Figure 26. Swirl Nozzle Performance, Nozzle Width 0.204 in.,
Nozzle Chord 1.33 in.

Figure 27. Diffuser Rotor Free Speeds

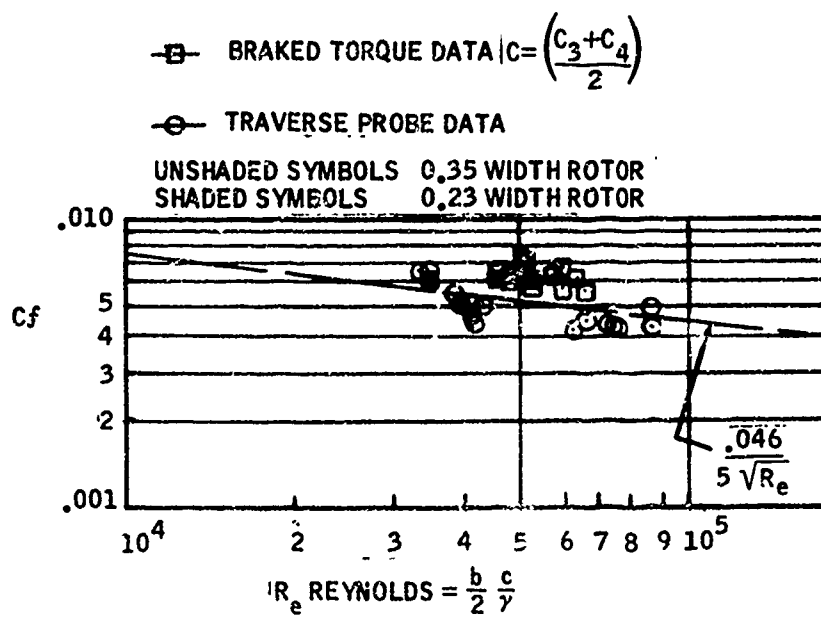Figure 28. Test Friction Coefficients

ROTOR DIAMETER RATIO 1.3
LOSS REDUCTION SHOWN INCLUDES CORRECTION
FOR ADDITIONAL STATIONARY FLOW PATH $\left(\dfrac{D_4}{D_3} \ 1.37\right)$
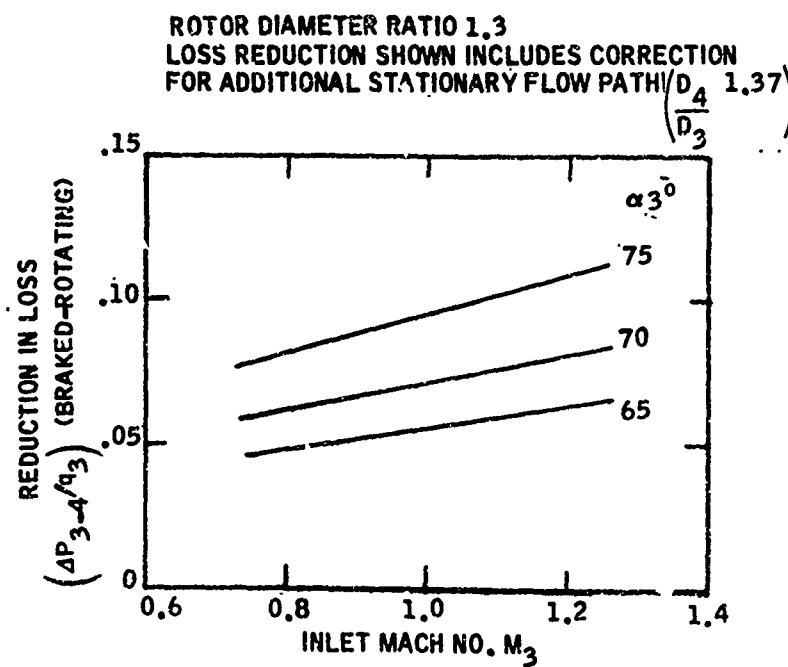
Figure 29. Estimated Performance, Rotating Vaneless Diffuser

APPENDIX 1

APPLICATION DESIGN STUDY

1. INTRODUCTION

A preliminary mechanical design study to examine methods of integrating the rotating vaneless diffuser into an advanced gas turbine generator set, with a high-pressure-ratio single-stage centrifugal compressor, was completed as part of the program work statement. A generator set with an output of 100 kW was studied with a design goal specific fuel consumption of 1.0 lb/kW-hr.

2. CYCLE CALCULATIONS

A turbine inlet temperature of 1500°F was selected for cycle calculations at standard sea level 60°F day conditions. This relatively low turbine inlet temperature is necessary in order to flat rate a 100 kW up to the extreme ambient condition of 5,000 feet altitude and 107°F, where the approximate turbine inlet temperature would be 1850°F.

Figure 30 shows the results of cycle calculations, where compressor efficiency is plotted versus pressure ratio with specific fuel consumption (SFC) as a parameter. In order to achieve the design goal SFC, a pressure ratio of 9.0 is required with a compressor adiabatic efficiency of 84%; substantially higher than is currently atta'nable with conventional single stage centrifugal compressors.

3. COMPRESSOR PERFORMANCE

The performance of 9.0:1 single stage centrifugal compressor designed for a specific ' ed NS = 65.0 (r.p.m., c.f.s$^{0.5}$, ft.$^{-0.75}$) with a supersonic free rotating vaneless diffuser followed by a subsonic vaned diffuser system was studied as a possible candidate configuration to meet the required efficiency level of 84%.

72

The moderately low specific speed was selected for compatibility with an existing MERDC designed 9. ᴄ:1 centrifugal compressor, with a rotating vaneless/vaned diffuser system, for which extensive impeller design information was available. Impeller efficiency was stipulated at 91.5% with a blading load distribution providing smooth outlet flow conditions at an absolute flow angle of 75 degrees (to radial). The estimated performance of the existing design impeller, mated with a free rotating vaneless supers sic diffuser, followed by a subsonic stationary diffuser, is shown in figure 31. This performance was computed assuming the losses in the free rotating diffuser were entirely frictional, with smooth entry and exit flow conditions; the subsequent subsonic stationary diffuser being therefore capable of attaining a static pressure recovery coefficient of 0.7. Figure 31 indicates that overall compressor efficiency increases significantly with increasing rotating diffuser diameter ratios up to to 1.3, after which the rate of efficiency increase diminishes. The rotating vaneless diffuser exit Mach number for a diameter ratio of 1.3 and a free speed ratio of 0.47 is comfortably subsonic at 0.85, with an estimated overall compressor adiabatic efficiency of 84.5%. A diffuser rotor diameter of 1.3 was therefore selected for further study.

4. ENGINE PERFORMANCE ESTIMATES

Detailed estimated performance of a 100 kW gas turbine generator set, with a single stage centrifugal compressor equipped with a 1.3 diameter ratio free rotating vaneless diffuser developing an overall pressure ratio of 9.0, is listed in Table 8. Estimated specific fuel consumptions at rated 100 kW output are 0.653 lb./hp.-hr. and 1.0 lb./kW-hr., with an alternator efficiency of 87.4%. Required compressor airflow is 2.1 lb./sec. which, with compressor specific speed of 63, results

73

in a required rotational speed of 61,400 r.p.m. Assuming a slightly lower diffuser free speed ratio U_3/C_{U_3} of 0.44 (to allow for as yet uncalculated bearing drag), the diffuser free rotational speed was calculated to be 24,100 r.p.m.

5. ROTATING DIFFUSER MECHANICAL DESIGN

To simplify the mechanical arrangement and to avoid unknown parasitic drag effects, it was decided early in the experimental rotating diffuser program that the front shroud would be supported from the rear shroud by small circular cross-section struts. Although the two shrouds need not necessarily be directly coupled, it still appeared that the strut support configuration lends itself best to simplicity of mechanical design and manufacturing, especially when considering integration into an actual gas turbine package. The struts, however, must be small in size to minimize drag, and yet robust enough to support the shroud under both steady state and transient operating conditions. For a diffuser diameter ratio of 1.3, the presence of struts tends to slightly increase the diffuser free rotating speed and helps to offset the retarding influence of the support bearing drag. The steady state stress in the circular struts is the sum of two bending stresses due to: (1) centrifugal bending of the strut under its own mass and (2) differential radial displacement of the two ends (shrouds) and axial distance between shrouds. Both stresses increase with speed but, at a given rotating diffuser speed, the centrifugal bending stress decreases and the end displacement stress increases with an increase in strut diameter. Circular strut stresses, calculated as a guided cantilever beam, are shown on figure 32 as a function of strut geometry of D/L^2 and diffuser tip speed. Optimum strut D/L^2

is 0.16, with a corresponding diameter of the order 0.01 inch for the design envisioned. Fabrication of the experimental diffuser showed that minimum strut diameters of the order 0.030 inch were necessary to ensure accurate and fixing; thus maximum diffuser tip speed would be limited to 750 fps, compared to a required tip speed for this design of 970 ft./sec. Elimination of the large displacement stresses in the strut is possible through uncoupling of the outer shrouds from the central disc; this could be achieved in several ways, one of which is shown in figure 36. The residual stress, if complete uncoupling were possible, would be the centrifugal bending of the strut due to its own mass, which is almost negligible.

An alternate approach to the strut stress problem would be to use an airfoil shaped strut or vane with a relatively high stiffness in the radial plane compared to a circular strut. The vane camber line would be ideally positioned along the calculated relative streamline path for the desired speed ratio, with a maximum thickness and fineness ratio providing no more drag than the circular struts. Development of the vane contour would be required in an actual compressor rig, since three dimensional flow would result in an incidence variation onto the vanes, thereby causing different sections of the vane to operate away from the desired "neutral" driving mode. The type of vane and diffuser geometry recommended is shown in figure 33 and could be manufactured by integral machining of the vanes with the front and rear shrouds. The airfoil vane approach would obviously be more practical for an actual gas turbine application and would avoid the high circular strut bending stresses at the expense of slightly more incidence sensitivity. The airfoil vane approach however, results in relatively

75

high stresses imposed on the vanes. A three dimensional finite element solution of the vane configuration, shown in figure 33, was therefore conducted to assess vane stresses. The three dimensional model was formed by taking a 25-degree sector of the two shrouds covering one vane spacing. Solid elements were used for the vanes and end fixing in the shrouds. Bending plate elements were used for the rest of the model. The inner diameter of the aft shroud was constrained with a fixed radial displacement to simulate a full disc. The average effective stress in the vane and shroud sector was 85,000 and 65,000 p.s.i. respectively at 24,100 r.p.m., for 17/4 PH stainless steel with a U.T.S. of 160,000 p.s.i. Some slight reduction of the strut stress problem is possible by decreasing the free rotational speed with either increasing frictional resistance on the diffuser outer shrouds or increased bearing drag. The estimated effect of bearing drag on free rotating speed ratio U_3/U_3 is shown on figure 34. Nominal bearing power is anticipated to be of the order 0.7 hp.; thus figure 34 indicates that relatively large increases in bearing drag are required in order to obtain a significant reduction in free speed ratio. A further disadvantage to this approach is that bearing drag materializes in oil heat; thus larger oil coolers would be required. Roughening of the stationary shrouds, is however, quite a practical approach to finesse the free speed ratio.

6. ENGINE ARRANGEMENTS

A conceptual 100 kW turboalternator arrangement, incorporating a single stage centrifugal compressor and a free rotating vaneless diffuser developing an overall stage pressure ratio of 9.0 with an efficiency of 84%, is shown in figure 35. The compressor is mounted back-to-back with a high-tip-speed single-stage radial-inflow turbine designed for an overall total-static efficiency of 85%. The free

rotating diffuser is mounted at its hub on preloaded matched duplex angular

contact ball bearings, sandwiched in between the compressor and turbine,

adjacent to the main shaft roller bearing. A staggered labyrinth seal is

placed on the rear disc of the rotating diffuser which, together with venting of

the forward and rear cavities to impeller tip pressure, reduces the axial end

thrust to a level compatible with bearing life requirements. The rotating diffuser

front shroud is supported by fifteen equally spaced "neutral" airfoil vanes

machined integral with the shrouds. Note that the rims of the rotating diffuser

do not require elaborate seals to prevent flow recirculation around the shrouds,

due to similar pressure gradients in the main core and side gaps. Decreasing

the free rotating speed to less than $U_3/C_{U_3} = 0.35$ would, however, probably require

rim seals.

An alternative turboalternator arrangement, using the same compressor and rotating

diffuser design coupled to a two-stage axial turbine, is shown in figure 36.

This shows a rotating diffuser construction with cir . ar support struts uncoupled

from the central disc by a flexible, annular, thin-shell section. An air bearing

support system for the rotating vaneless diffuser was briefly examined and

discarded owing to its cost and complexity. A three-pad support was envisioned

equally spaced around the circumference and fed with compressor discharge air

(after all diffusion was completed). Drawbacks to the scheme were leakage of

high pressure air back to the impeller tip and a large variation of radial gap

between the diffuser and support pad with changes in diffuser speed. It was

therefore required to consider spring loaded air bearing pads floating with the

radial excursions of the diffuser.

A third conceptual turboalternator arrangement is shown in figure 37, which probably represents the ultimate in performance for a "single" stage centrifugal compressor. The rotating diffuser, compressor rotor front shroud, and first stage inducer are integrated into a single unit susperded by a front bearing system concentric with the main inner shaft. No attempt was made to assess the mechanical feasibility of this system, since accurate finite element modeling of the complex outer rotor system would require extensive time in order to arrive at stress and distortion information. The arrangement is presented to indicate the possible trends in advanced centrifugal compressor design The rotating diffuser and inducer blading would be designed to operate at optimum speed ratio which is calculated to be near 0.4, under which conditions the diffuser vanes would be extracting power to drive the inducer. The relative Mach numbers throughout the rotor flow path could be kept as low as 0.7 at stage pressure ratios up to 10:1.

Examination of the various turboalternator arrangements reveals that performance improvements will not be obtained without increases in complexity and probably cost. Advanced manufacturing techniques and materials development, however, will serve to minimize these effects, such that rotating diffuser systems for centrifugal compressors can establish a practical position in turbomachinery engineering.

7. SYSTEM ROTOR DYNAMICS

The preliminary gas turbine engine design incorporating a free rotating diffuser, shown in figure 35, was reviewed with regard to system dynamics.

The rotating diffuser rotor is mounted on a duplex pair of bearings mounted back-to-back, providing inwardly diverging contact angle lines. This bearing arrange-

78

ment provides high angular rigidity and should limit rotor excursions. Figure 38 gives the particulars for the diffuser rotor dynamics. The critical speed is 38,900 r.p.m. and the dynamic response with 0.003 ounce-inch unbalance is given for three speeds. Both the bearing loads and radial excursion are quite low in the expected operating speed range of the diffuser.

The engine main rotor is supported on a ball and roller bearing combination, with the turbine over-hung and the compressor straddle mounted. This rotor-bearing configuration is a departure from normal Solar practice, but has been used by other turbine manufacturers. Figure 39 shows the dynamic response of the rotor over the full range of running speed. The first and second criticals occur at 38,400 r.p.m. and 91,300 r.p.m. respectively. Bearing loads given apply for in-phase unbalance of 0.003 ounce-inch in the two balance planes of the compressor and turbine rotors. Radial excursion of the turbine exducer tip is also given at the first critical and at the 62,000 r.p.m. operating speed.

SYSTEM BEARING LIFE

Data from the dynamic response calculations were utilized to estimate the following bearing lives:

Diffuser Rotor

B_{10} Life = 8200 Hours

Main Rotor Bearings

Ball B_{10} Life = 5200 Hours

Roller B_{10} Life = 8350 Hours

All computed life figures apply for M-50 tool steel material.

8. DIFFUSER LAG DURING STARTING

During starting, the rotating diffuser speed will lag behind that of the main rotor assembly from which it is mechanically independent. The lag will depend upon the inertia of the diffuser, bearing drag, and strut aerodynamic characteristics. Assuming that the latter two effects are relatively small, the speed lag of the diffuser during start can be readily calculated for a known acceleration rate of the main rotor assembly. Figure 40 shows that with a linear acceleration rate of the main rotor from zero to rated speed, say 60 seconds, that the diffuser will reach rated speed 10 to 50 seconds later, dependent upon its inertia. The estimated polar moment of inertia for the rotating vaneless diffuser config ion shown in figure 35 is 0.01 lb.ft.sec.^{2}. Speed excursions of the diffuser during on-off load transients will be negligible, since at constant impeller speed the variation of inlet Mach number and flow angle with load is small.

9. SUMMARY OF DESIGN STUDY

The concept of integrating the free rotating vaneless diffuser in an advanced 100 kW gas turbine generator set is feasible and will provide performance improvements at the expense of increased cost and complexity. The recommended mechanical arrangement is that shown in figure 35, where the diffuser is supported by a central antifriction bearing system. The fr   shroud is attached to the rear disc by fifteen airfoil shaped "neutral" vanes. Average vane stress at design speed of 24,100 r.p.m. is computed to be 0.5 material U.T.S. Aerodynamic and mechanical development of these vanes will require separate compressor rig testing.

It is estimated that the free rotating diffuser will reach equilibrium speed 35% later than the time the main rotating assembly attains rated speed. Speed excursions of the diffuser during on-off load transients will be negligible.

10. RECOMMENDATIONS

. Development of the free rotating vaneless diffuser should be continued to the stage of evaluating its performance characteristics in an actual high-pressure-ratio centrifugal-compressor rig.

. The rotating diffuser configuration recommended for test is an integrally machined assembly with fifteen (or more) airfoil shaped "neutral" support vanes.

. A rotating diffuser configuration, as sized in the design study, could be readily incorporated into a new compressor rig being developed by MERDC.

TABLE 8

ADVANCED 100 KW GENERATOR SET CYCLE ANALYSIS, SEA LEVEL AND 60°

Main Rotor Speed	r.p.m.	61,400
Free Rotating Diffuser Speed	r.p.m.	24,100
Compressor Air Flow	lb./sec.	2.10
Compressor Pressure Ratio		9.0
Compressor Efficiency	%	84.0
Inlet Heating	°F	10
Combustor Pressure Drop	%	3
Exhaust Pressure Drop	%	2
Inlet Pressure Drop	%	1
Turbine Inlet Temperature	°F	1500
Turbine Exhaust Temperature	°F	814
Turbine Efficiency	%	85
Burner Efficiency	%	97
Mechanical Efficiency	%	95
Alternator Efficiency	%	87.4
Output Power	hp.	153.5
SFC	lb./hp.-hr.	0.653
SFC	lb./kW-hr.	1 0
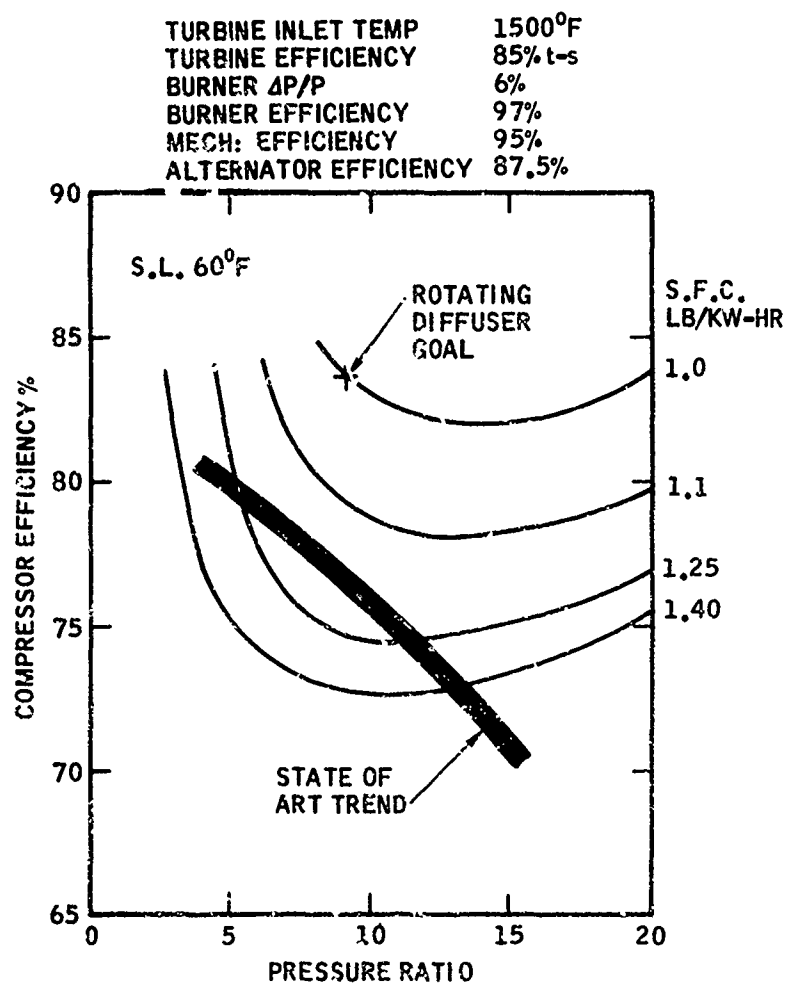
Figure 30. Effect of Compressor Efficiency on Specific Fuel Consumption

OVERALL PRESSURE RATIO 9.0
IMPELLER EFFICIENCY 91.5%
ABSOLUTE AIR ANGLE IMPELLER TIP 75°
STATIONARY DOWNSTREAM DIFFUSER Cp 0.7
SPECIFIC SPEED $N_S = 65$
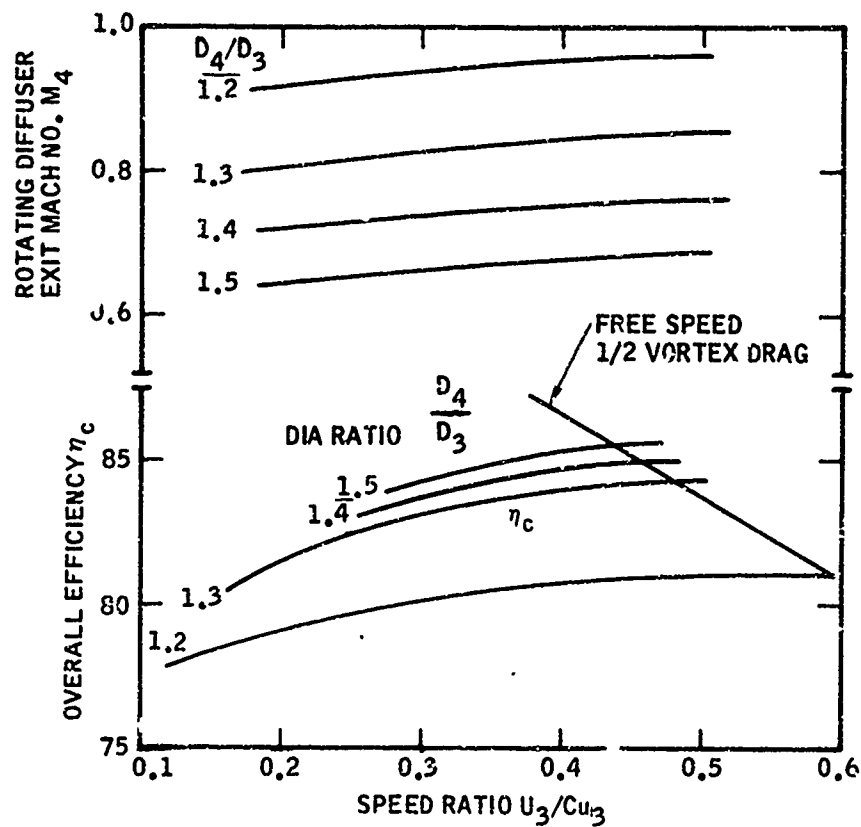
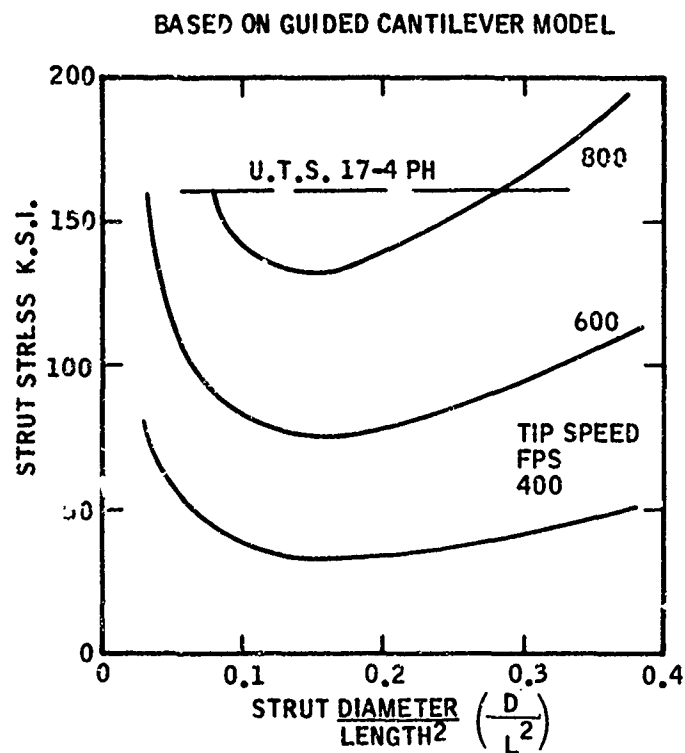Figure 31. Estimated Efficiency, Rotating Vaneless Diffuser Compressor

BASED ON GUIDED CANTILEVER MODEL

Figure 32. Rotating Diffuser Circular Strut Stresses

15 VANES

STATIONARY
DIFFUSER

25° STRESS SECTOR

12.0 DIA

9.10 DIA

7.0 DIA

ROTATING DIFFUSER
ASSY. WITH INTEGRAL
"NEUTRAL" VANES
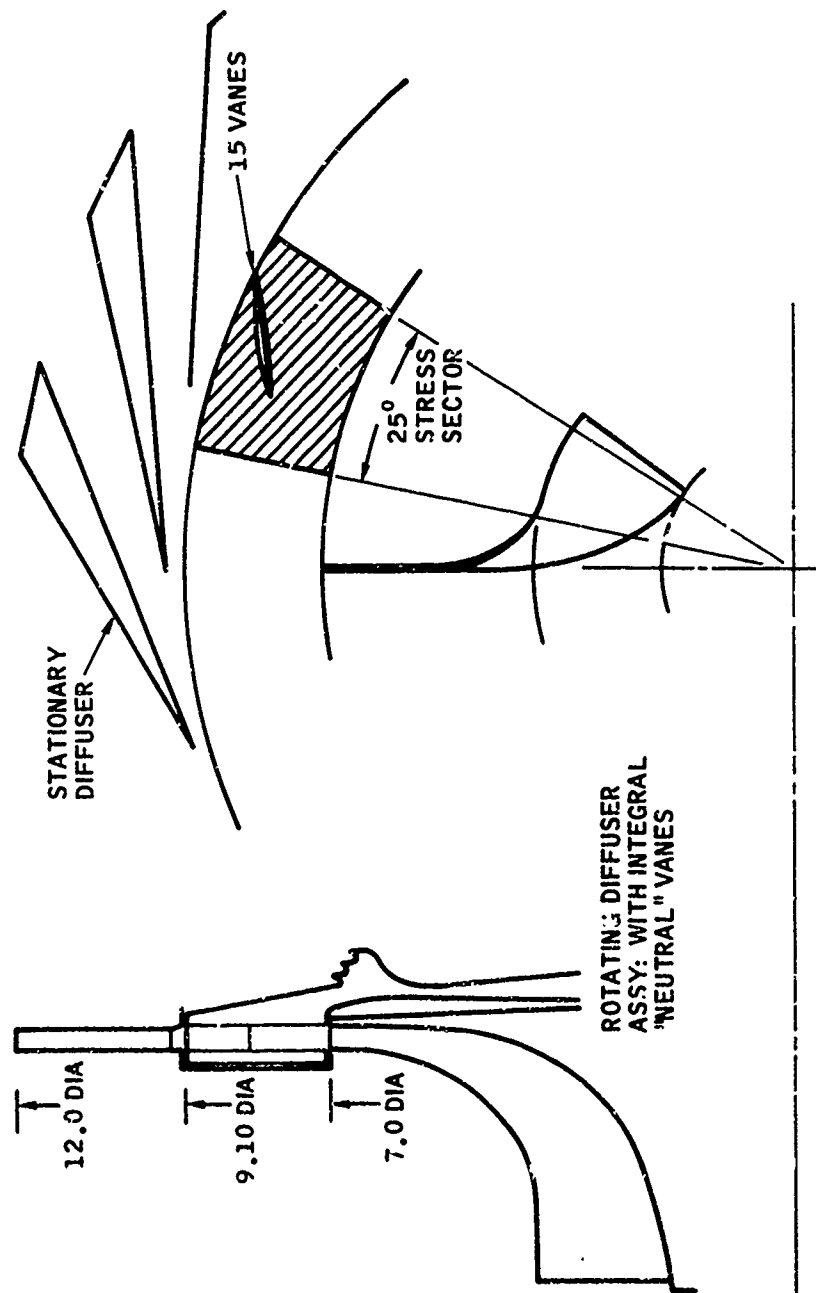
Figure 33.   Rotating Diffuser Assembly with Integral "Neutral" Vanes
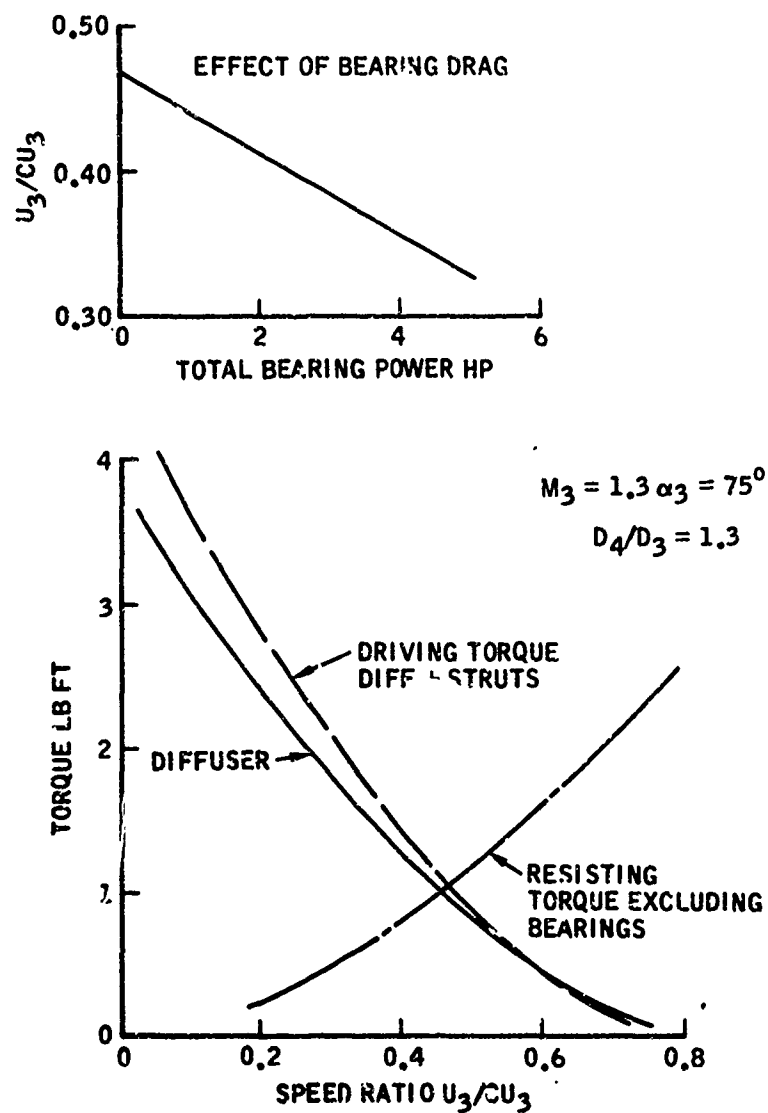
Figure 34. Free Rotating Diffuser Estimated Torque Curve
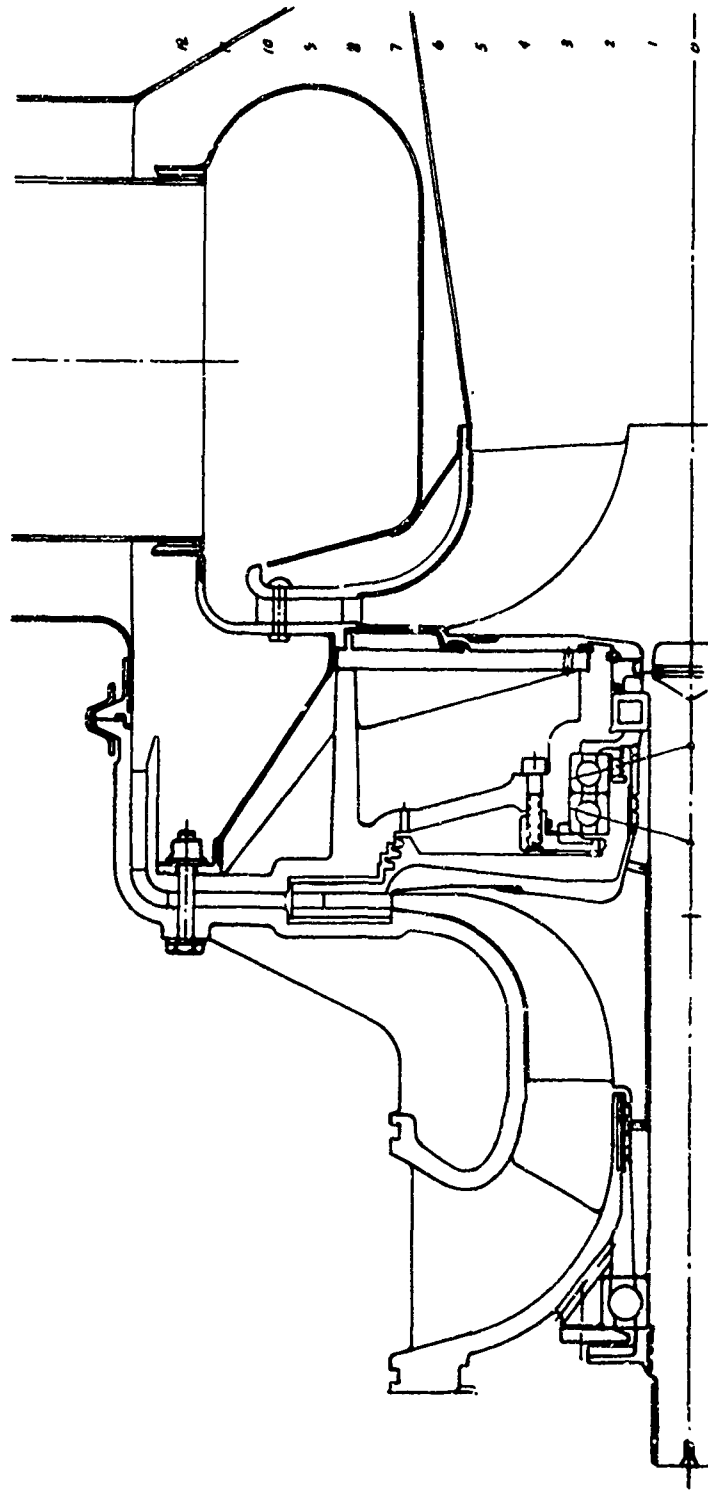
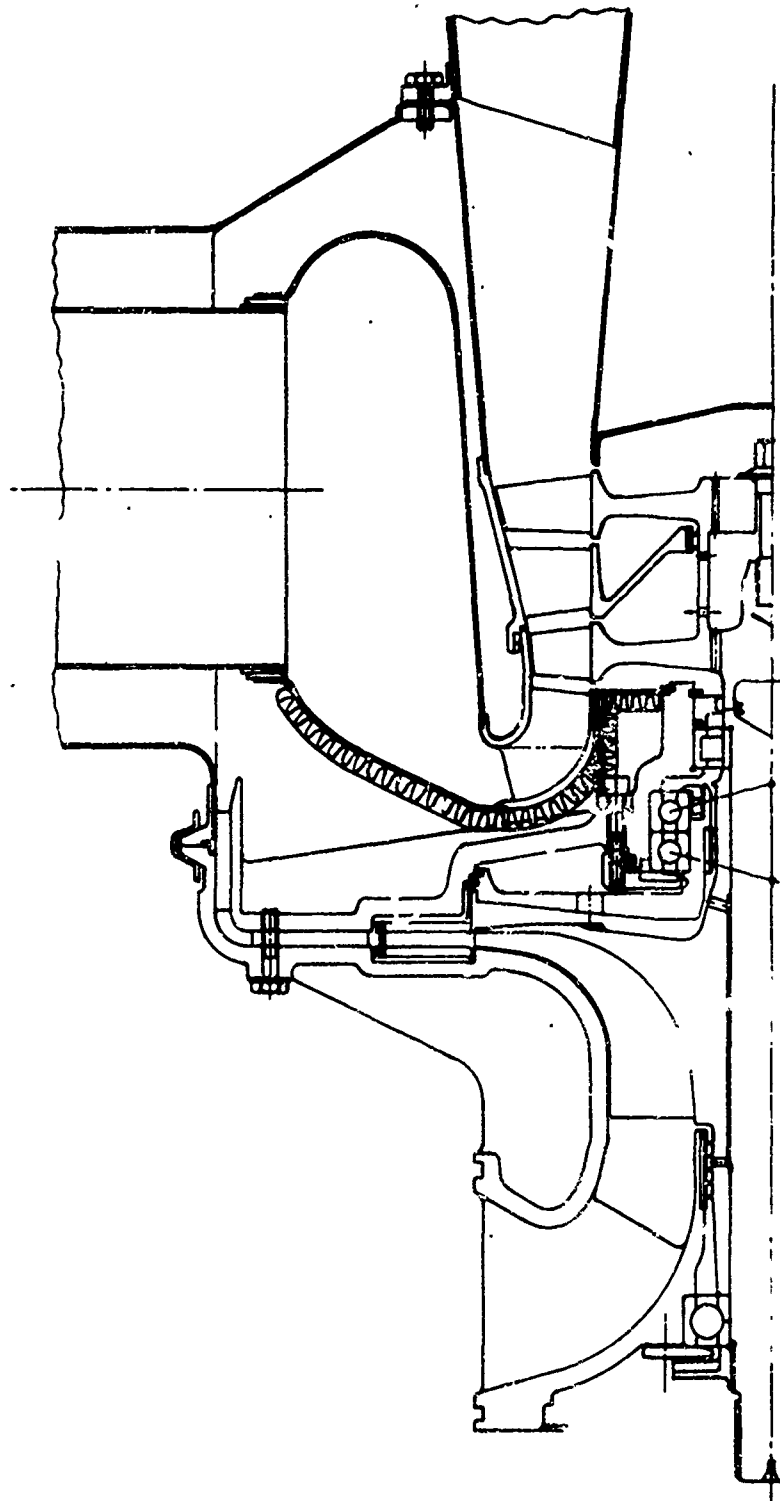Figure 35. Conceptual Gas Turbine Design with Free Rotating Diffuser, Radial Turbine

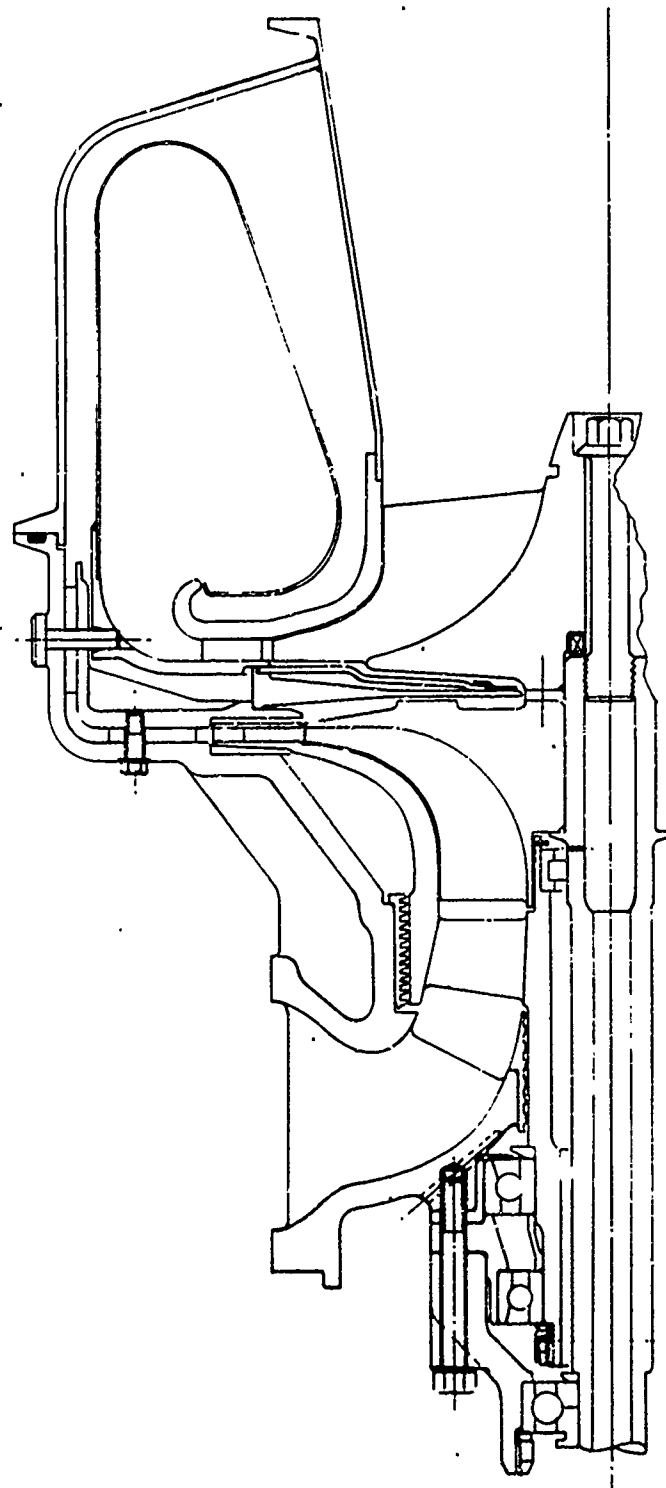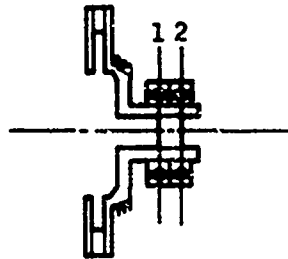Figure 36. Conceptual Gas Turbine Design with Free Rotating Diffuser, Axial Turbine

Figure 37. Conceptual Gas Turbine with Free-rotating Inducer/Diffuser Combination

CRITICAL SPEED = 38,900 RPM
UNBALANCE = .003 OZ-IN IN TWO PLANES

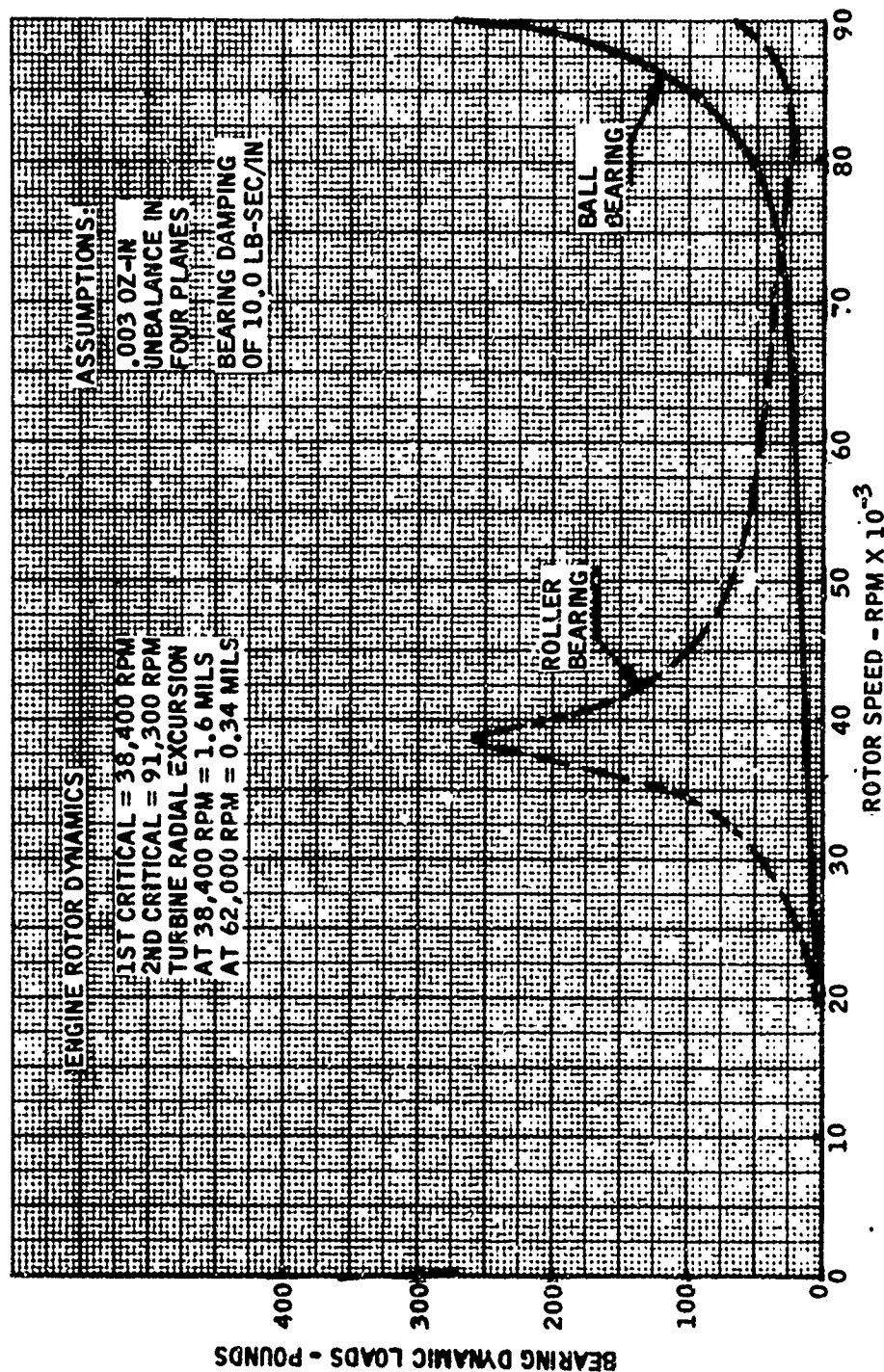|	15,000 RPM	17,500 RPM	20,000 RPM
NO. 1 BRG. LOAD, LBS.	1.2	1.9	2.8
NO. 2 BRG. LOAD, LBS.	2.1	2.9	3.9
RADIAL EXCURSION MILS	.010	.013	.020

Figure 38. Diffuser Rotor Dynamics

Figure 39. Engine Rotor Dynamics
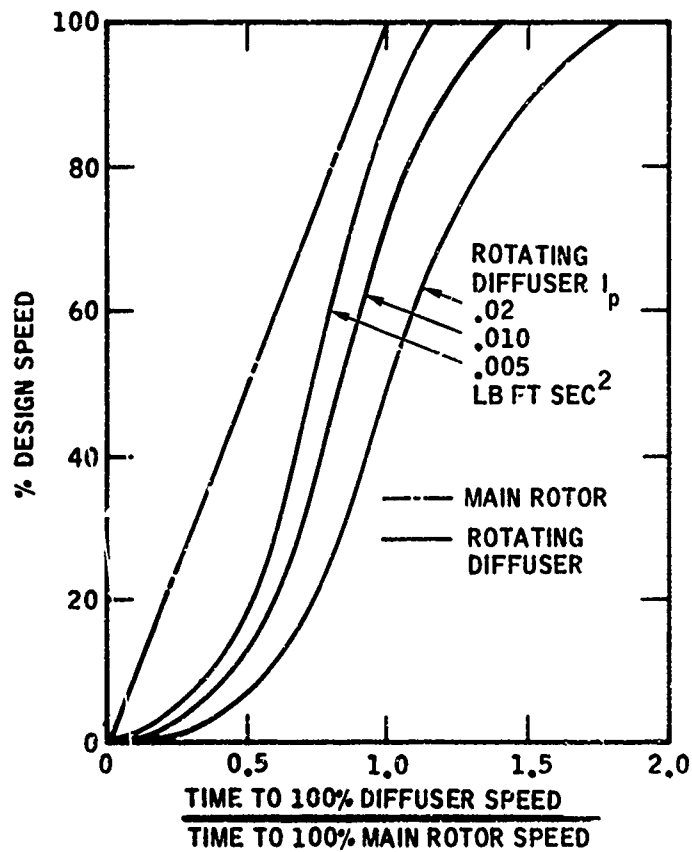
NOTE TYPICAL MAIN ROTOR I_p .004-.010 LB FT SEC^2

Figure 40. Estimated Starting Transient, 100kW Gas Turbine with
Free-rotating Diffuser

APPENDIX 2
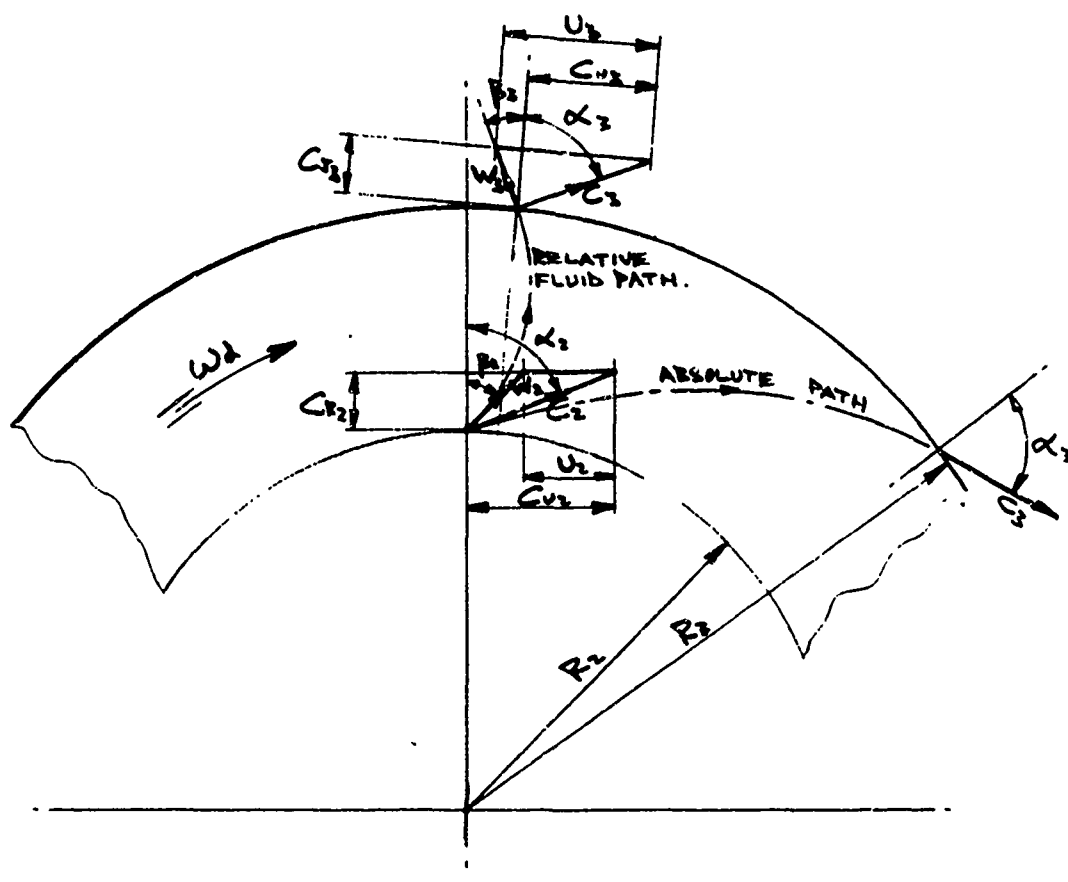
ROTATING VANELESS DIFFUSER COMPUTER PROGRAM

Figure 41. Rotating Diffuser: Geometry of Flow Path for
Theoretical Analysis

C.S.M.P. - ROTATING VANELESS DIFFUSER
COMPUTER PROGRAM NOMENCLATURE

ALF	α ABSOLUTE FLOW ANGLE	OUTPUT
AL2	α_2 INLET ABSOLUTE FLOW ANGLE	INPUT
BR2	b/r_2 WIDTH / RADIUS	INPUT
CA	$(\gamma-1) M_{c2}^2 / (1+ \cot^2\alpha_2)$	
CB	$-CT/(b/r_2)$	
CC	$\gamma M_{c2}^2 \cot\alpha_2 / (1+ \cot^2\alpha_2)$	
CD	$\gamma-1$	
CE	$1+ \cot^2\alpha_2$	
CF	FRICTION COEFFICIENT	INPUT
CTA	$\cot\alpha$	
CTA2	$\cot\alpha_2$	
DMNCTA	$\partial(\mu\nu \cot\alpha)/\partial\mu$	
DMUNU	$\partial(\mu\nu)/\partial\mu$	
DPSP2	$\partial(p/p_2)/\partial\mu$	
GAM	γ SPECIFIC HEAT RATIO	INPUT
LAM	λ SPEED RATIO	INPUT
ITR	$(\mu\nu-1)$ TORQUE RATIO	OUTPUT
MC	M_c ABSOLUTE MACH Nº	INPUT
MC2	M_{c2} INLET ABSOLUTE MACH Nº	
MC2S	M_{c2}^2	

MNCTA	$\mu\nu\cot\alpha$	
MU	μ RADIUS RATIO	OUTPUT
MUNU	$\mu\nu$	
NCTA	$\nu\cot\alpha$	
NU	$\nu = Cu/Cu_2$ TANGENTIAL VELOCITY RATIO	
PPS	P/p PRESSURE RATIO	
PPS2	P/p_2 " "	
PSP2	p/p_2 " "	
SPLC	$(P_2-P)/(P_2-p_2)$ PRESSURE LOSS COEFF	OUTPUT
SPRC	$(p-p_2)/(P_2-p_2)$ STATIC PRESSURE RECOVERY	OUTPUT
TRR	$(T-T_2)/T_2$ TEMP RISE RATIO	OUTPUT
TR2	T_2/t_2 TEMP RATIO	
TST2	t/t_2 TEMP RATIO	
TTS	T/t TEMP RATIO	
TTT2	T/t_2 TEMP RATIO	
VA	$\nu-\lambda\mu$	
VB	$(\nu-\lambda\mu)/\nu\cot\alpha$	
VC	$\nu^2(1+\cot^2\alpha)$	
XMNCTA	NUMERATOR OF DMNCTA	

$$\frac{\partial (\mu\nu)}{\partial \mu} = -\frac{C_f}{(b/r_2)}\mu(\nu-\lambda\mu)\left[1+\left(\frac{\nu-\lambda\mu}{\nu\cot\alpha}\right)^2\right]^{1/2}$$

$$\frac{\partial(\mu\nu\cot\alpha)}{\partial\mu} = \left(\frac{M_{c2}^2}{1+\cot^2\alpha_2}\right)\nu\cot\alpha\left\{\frac{\left[\nu^2(1+\cot^2\alpha)+(\gamma-1)(\nu-\lambda\mu)+\frac{\gamma\nu^2\cot^2\alpha}{\nu-\lambda\mu}\right]\frac{\partial(\mu\nu)}{\partial\mu}}{\left\{\nu^2\cot^2\alpha\left(\frac{M_{c2}^2}{1+\cot^2\alpha_2}\right)-\frac{t}{t_2}\right\}}\right\}$$

$$\frac{\partial(b/r_2)}{\partial\mu} = \frac{\gamma}{\mu^2}\left(\frac{M_{c2}^2}{1+\cot^2\alpha_2}\right)\cot\alpha_2\left[\frac{\nu^2(1+\cot^2\alpha)}{\nu\cot\alpha}+\frac{\nu\cot\alpha}{(\nu-\lambda\mu)}\frac{\partial(\mu\nu)}{\partial\mu}-\frac{\partial(\mu\nu\cot\alpha)}{\partial\mu}\right]$$

$$\frac{t}{t_2} = \frac{T}{t_2}-\frac{(\gamma-1)}{2}\left(\frac{M_{c2}^2}{1+\cot^2\alpha_2}\right)\nu^2(1+\cot^2\alpha)$$

$$\frac{T}{t_2} = \frac{T_2}{t_2}+\frac{\Delta T_i}{t_2} \quad ; \quad \frac{T_2}{t_2} = 1+\frac{(\gamma-1)}{2}M_{c2}^2 \quad ; \quad \frac{P_2}{p_2} = \left(\frac{T_2}{t_2}\right)^{\frac{\gamma}{\gamma-1}}$$

$$\frac{\Delta T_i}{t_2} = (\gamma-1)\left(\frac{M_{c2}^2}{1+\cot^2\alpha_2}\right)\lambda(\mu\nu-1)$$

$$P/p = \left[(T/t_2)/(t/t_2)\right]^{\gamma/\gamma-1}$$

$$\frac{P}{P_2} = \left(\frac{P}{p}\right)\left(\frac{p}{P_2}\right)$$

$$\frac{P_2-P}{P_2-p_2} = 1-\frac{(P/p_2)-1}{(P_2/p_2)-1}$$

$$\frac{\Delta T_e}{t_2} = \frac{1}{5}\frac{C_f^{p'}}{(b/r_2)}\left(\frac{\rho'}{\rho_2}\right)\frac{f^2\lambda^3}{\cot\alpha_2}\frac{(\gamma-1)M_{c2}^2}{(1+\cot^2\alpha_2)}\quad(\mu\leq1)$$

f = Vortex tangential speed ratio between rotating
and stationary shrouds

Equilibrium reached when $\frac{\Delta T_i}{t_2} = \frac{\Delta T_e}{t_2}$

ROTATING VANELESS DIFFUSER- COMPRESSIBLE FLOW

```
INITIAL
      CB=-CF/BR2
      CD=GAM-1.
      CTA2=1./TAN(AL2/57.296)
      MC2S=MC2*MC2
      CE=1.+CTA2*CTA2
      CA=CD*MC2S/CE
      CC=GAM*MC2S*CTA2/CE
      TR2=MC2S*CD/2.+1.
      PPS2=TR2**(GAM/CD)
DYNAMIC
      MU=TIME+1.
      NU=MUNU/MU
      NCTA=MNCTA/MU
      CTA=NCTA/NU
      ALF=57.296*ATAN(1./CTA)
      MC=SQRT(2./CD*(TTS-1.))
      PPS=TTS**(GAM/CD)
      SPLC=(PPS2-PPS*PSP2)/(PPS2-1.)
      ITR=MUNU-1.
      TTT2=TR2+CA*LAM*ITR
      TST2=TTT2-CA*VC/2.
      TTS=TTT2/TST2
      TRR=TTT2/TR2-1.
      SPRC=(PSP2-1.)/(PPS2-1.)
      DMUNU=CB*MU*VA*SQRT(1.+VB*VB)
      VA=NU-LAM*MU
      VB=VA/NCTA
      VC=NU*(NU+NCTA*CTA)
      XMNCTA=MC2S*NCTA*(VC+DMUNU*(CD*VA+GAM*NCTA/VB))
      DMNCTA=XMNCTA/(NCTA*NCTA*MC2S-TST2*CE)
      DPSP2=CC/MU/MU*(VC/NCTA+DMUNU/VB-DMNCTA)
      MUNU=INTGRL(1.,DMUNU)
      MNCTA=INTGRL(CTA2,DMNCTA)
      PSP2=INTGRL(1.,DPSP2)
METHOD RKSFX
TIMER DELT=.005,PRDEL=.1,FINTIM=1.
PRINT MU,ALF,MC,SPLC,SPRC,TRR,ITR
PARAM GAM=1.395
PARAM AL2=65.
PARAM CF=.005
PARAM LAM=(0.,.2,.4,.6)
PARAM BR2=.1167
PARAM MC2=.8
TITLE ROTATING VANELESS DIFFUSER - COMPRESSIBLE FLOW.
PARAMETER STUDY. END
```

100